

International Atomic Energy Agency

INDC(CCP)-31/U

---

**INDC**

**INTERNATIONAL NUCLEAR DATA COMMITTEE**

---

NUCLEAR PHYSICS RESEARCH IN THE USSR

(Collected Abstracts)

No.11

Translated by the IAEA  
December 1972

---

**IAEA NUCLEAR DATA SECTION, KÄRNTNER RING 11, A-1010 VIENNA**



USSR STATE COMMITTEE ON THE UTILIZATION OF ATOMIC ENERGY  
NUCLEAR DATA INFORMATION CENTRE

NUCLEAR PHYSICS RESEARCH IN THE USSR  
(Collected Abstracts)  
No.11

English translation of an original in Russian published by  
Atomizdat, 1970



EDITORIAL BOARD

V.A. KUZNETSOV (Chief Scientific Editor), Yu.V. ADAMCHUK,  
V.N. ANDREEV, G.Z. BORUKHOVICH, V.P. ZOMMER, D.A. KARDASHEV  
(Editor-in-Chief), I.A. KORZH, V.A. NAUMOV, A.I. OBUKHOV and  
Yu.P. POPOV



I.V. KURCHATOV ATOMIC ENERGY INSTITUTE

ANGULAR DISTRIBUTIONS OF FRAGMENTS AND THE CROSS-SECTION OF  $^{249}\text{Bk}$   
FISSION BY NEUTRONS

P.E. Vorotnikov, S.M. Dubrovina, V.N. Kosyakov, G.A. Otroshchenko,  
L.V. Chistyakov, V.A. Shigin and V.M. Shubko

The measurements were performed in an electrostatic accelerator. The fragments were recorded with glasses. In the processing of the results, a correction was made for the beta-decay of  $^{249}\text{Bk}$  with a half-life of 314 days and for the background due to the fission of the accumulating  $^{249}\text{Cf}$ . The table of cross-sections gives the relative measurement error. The standardization error is about 10%.

Table 1. Fission cross-section of  $^{249}\text{Bk}$

$E_n$ keV	$\bar{\sigma}$ , barn	$\Delta \bar{\sigma}$ barn
650	0,009	0,01
700	0,031	0,01
750	0,075	0,01
800	0,096	0,01
850	0,17	0,015
900	0,22	0,015
950	0,41	0,02
1000	0,53	0,02
1050	0,65	0,03
1100	0,81	0,01
1150	0,85	0,03
1200	0,99	0,03
1250	0,97	0,02
1300	1,06	0,03
1350	1,15	0,03
1400	1,16	0,03
1500	1,20	0,02
1550	1,32	0,03
1600	1,31	0,03
1650	1,38	0,03
1700	1,41	0,03
1800	1,37	0,05
4,6 MeV	1,50	0,05

Table 2. Angular distribution of  $^{249}\text{Bk}$  fission fragments

$E_n$	$0^\circ/90^\circ$	$30^\circ/90^\circ$	$60^\circ/90^\circ$	$\Delta$
1000	1,15	1,033	1,035	$\pm 0,06$
1200	1,09	1,10	1,021	$\pm 0,045$
800	1,07	0,77	1,11	$\pm 0,15$
1400	1,05	1,06	1,028	$\pm 0,045$
1600	1,127	1,18	1,07	$\pm 0,04$
4600	1,06	1,086	1,003	$\pm 0,04$



STUDY OF A POSSIBLE CASE WHERE NON-DEPENDENCE OF COMPOUND NUCLEUS  
DECAY ON ENTRANCE CHANNEL SPIN DOES NOT HOLD

K.V. Karadzhev, V.I. Manko, A.N. Nersesyan and F.E. Chukreev

The anisotropy of the angular distribution of gamma-rays from the  $^{31}\text{P}(p, \gamma_0)^{32}\text{S}$  reaction was measured in the resonance region with an energy of 2114 keV. The spin mixing co-efficient  $t = 0.98$  obtained here agrees satisfactorily with that determined for this resonance from the  $^{31}\text{P}(p, \alpha)^{28}\text{Si}$  and  $^{31}\text{P}(p, p)^{31}\text{P}$  reactions [2].

CALCULATIONS OF THE CROSS-SECTIONS FOR THE ELASTIC- AND INELASTIC-  
SCATTERING OF 0.3-1.5 MeV NEUTRONS BY ATOMIC NUCLEI

I.K. Averianov, A.E. Saveliev and B.M. Dzyuba

(Submitted to Bjulleten CJAD GKAE<sup>8</sup> (Bulletin of the Nuclear Data  
Centre of the USSR State Committee on the Utilization of Atomic  
Energy) No. 7 (1971))

The authors performed calculations of the differential cross-sections for the elastic- and inelastic-scattering of 0.3-1.5 MeV neutrons by different atomic nuclei with  $A = 23-238$ . The calculations were based on the optical model of elastic neutron scattering and on the Hauser-Feshbach method of calculating the elastic- and inelastic-scattering cross-sections of neutrons in terms of a compound nucleus.

The available experimental data can be described satisfactorily with the optical-potential parameters obtained. On the basis of these parameters it is possible to predict, with a certain degree of accuracy, the differential elastic- and inelastic-scattering cross-sections of neutrons by nuclei, for which the relevant experimental data are absent.

INSTITUTE OF PHYSICS AND POWER ENGINEERING

DENSITY OF EXCITED STATES OF ATOMIC NUCLEI

A.V. Ignatyuk, V.S. Stavinsky  
and Yu. N. Shubin

(Paper presented at the 2nd International Conference  
on Nuclear Data for Reactors, Helsinki, 1970)

In order to evaluate average neutron cross-sections, it is necessary to have detailed and reliable information on the widths of the processes involved. In statistical theories of nuclear reactions these are expressed in terms of the excited state density of the final reaction products. Since high degrees of accuracy and reliability are required in evaluating reactor constants, it is essential to develop new methods of calculating the energy dependence of nuclear level density. The average values of excited nuclei and of neutron cross-sections cannot be represented consistently with the generally accepted Fermi-gas model. The paper discusses the results of calculations of the level density of atomic nuclei, in which systematic account is taken of the individual properties of nuclei associated with their shell structure. The calculations are based on the superfluid-nucleus model, which is at present being used with success in analysing the properties of low-lying excited states of nuclei. The calculations do not involve the use of additional parameters and provide a means based on a single approach for correlating the properties of highly excited nuclei and those of nuclei in the ground and weakly excited states. The calculations performed show that the discrete structure of the single-particle spectrum leads to substantial changes in the energy dependence of level density as compared with the Fermi-gas model, provides a natural explanation for the anomalies observed in the spectra of inelastically scattered neutrons and yields a qualitative description of the main characteristics of the nuclear fusion process, phase-transition range and so on. The spin dependence of nuclear level density and the dependence of the equilibrium deformation of nuclei on excitation energy are also considered. The internal consistency of the model and the fact that it explains the different average characteristics of excited nuclei justify the hope that the proposed method will provide a reliable basis for calculating and evaluating nuclear data.

THE STATISTICAL PROPERTIES OF THE SPECTRA OF ATOMIC NUCLEI AT LOW  
EXCITATION ENERGIES

Yu.V. Sokolov and V.S. Stavinsky

(Preprint, Institute of Physics and Power Engineering)

The paper presents a theoretical analysis of the energy dependence of the level density of  $^{41}\text{Ca}$ ,  $^{50}$ ,  $^{51}$ ,  $^{52}$ ,  $^{54}$ ,  $^{55}\text{Cr}$ ,  $^{58}$ ,  $^{59}\text{Fe}$  and  $^{56}\text{Mn}$  nuclei obtained from the (pp') and (dp) reactions. For this purpose, a refined Fermi gas model is used with phenomenological treatment of the residual interactions.

Possible reasons for the deviation of predictions by this simple model from the experimental data are discussed briefly.

STATISTICAL DESCRIPTION OF RADIATION WIDTHS

A.V. Ignatyuk

(Submitted to *Jadernaja Fizika*)

The paper considers the influence of the shell structure of the spectrum of single-particle states of nucleons on the behaviour of the average radiation widths of excited nuclei. The gamma-ray spectra obtained and the dependence of radiation width on excitation energy differ considerably from the results of the statistical description of Weisskopf.

THE ACCURACY OF ASYMPTOTIC EXPRESSIONS FOR THE DENSITY OF EXCITED  
NUCLEAR STATES

A.V. Ignatyuk

(Submitted to Physics Letters)

An asymptotic series determining the density of the excited states of a confined Fermi gas is obtained in the analytical form. The main term in this series coincides with the expression generally used for level density, the subsequent terms permitting determination of the accuracy of this expression.

THE STRUCTURE OF A SINGLE-PARTICLE SPECTRUM AND THE ENERGY  
DEPENDENCE OF  $\Gamma_f/\Gamma_n$

A.V. Ignatyuk, G.N. Smirenkin  
and A.S. Tishin

(Paper presented at the Second International Conference  
on Heavy Ions, Dubna 1971)

In the analysis of experimental data,  $\Gamma_f/\Gamma_n$  is generally described in terms of the well-known relations of the Fermi gas model, in accordance with which the level density parameters  $a$  are independent of excitation energy.

The paper considers the contradictory nature of these results. It shows that in describing neutron width one has to take into account the influence of the shell structure of the single-particle spectrum on the behaviour of the level density parameter. Allowance for the dependence of parameter  $a$  on excitation energy results in an appreciable change in the fission barrier value for "light" nuclei derived from the analysis of  $\Gamma_f/\Gamma_n$ .

PARAMETERS OF THE MULTILEVEL ANALYSIS OF  $^{239}\text{Pu}$  CROSS-SECTIONS  
IN THE RESONANCE REGION

A.A. Lukyanov

(Paper presented at the French-Soviet Seminar  
Dubna, 1970)

On the basis of the S-matrix formalism, the total and fission cross-sections of  $^{239}\text{Pu}$  are parametrized in the region below 100 eV with allowance for the effects of interresonance interference. The results obtained in various studies are compared and the main properties of the parameters responsible for the interference are discussed.

COUPLED CHANNEL SCHEME IN THE R-MATRIX FORMALISM

A.A. Lukyanov

(Submitted to *Teoretičeskaja i Matematičeskaja Fizika*)

In the formal theory of nuclear reactions with nucleons, the collision matrix is subdivided into bound and decaying base states respectively. Assigning the sense of the matrix of the direct interactions to one part and that of the resonance matrix of the compound nucleus to the other, the paper considers the structure of the widths of the bound states and the complex potential model.

CROSS-SECTIONS FOR THE RADIATIVE CAPTURE OF NEUTRONS BY THORIUM-232  
AND URANIUM-238 NUCLEI

Yu.Ya. Stavissky and V.A. Tolstikov

(Submitted to *Bjulleten CJaD GKAE* No. 7 (1971))

The paper presents measurements of averaged cross-sections for the radiative capture of neutrons by  $^{232}\text{Th}$  and  $^{238}\text{U}$  in the energy region below ~50 keV. They were made with a neutron spectrometer, on the basis of slowing-down time in lead. The energy dependence of the cross-sections is normalized to the resolved low resonances and radiative capture cross-sections for Ag and  $^{197}\text{Au}$ , which were measured in the present study.

The measurements were used to obtain the ratios of the radiative capture cross-sections of  $^{232}\text{Th}$  and  $^{238}\text{U}$  to the fission cross-sections of  $^{235}\text{U}$  and  $^{239}\text{Pu}$  measured earlier with a spectrometer on the basis of the slowing-down time.

The data of the present study are compared with the results of other authors.

REAPPRAISAL OF THE CROSS-SECTIONS FOR THE RADIATIVE CAPTURE  
OF NEUTRONS BY URANIUM-238

(December 1970)

A.I. Abramov and V.A. Tolstikov

(Preprint, Institute of Physics and Power Engineering)

Several new papers have appeared recently on the measurement and evaluation of the cross-sections for the radiative capture of neutrons by uranium-238 nuclei, data which supplement the information contained in Ref. [1].

In the present study, the new data were used as a basis for reappraising our earlier data, and new recommended values of  $\sigma_{\gamma}(^{238}\text{U})$  in the 0.001-14 MeV energy range were obtained.

REFERENCE

- [1] ABAGYAN, L.P., ABRAMOV, A.I., NIKOLAEV, M.N., STAVISSKY, Yu.Ya.,  
TOLSTIKOV, V.A., Nuclear Data for Reactors (Proc. Conf. Helsinki  
1970) 2 IAEA (1970) 667.

THE ENERGY SPECTRA OF INELASTICALLY SCATTERED NEUTRONS FOR THE CASE  
OF CHROMIUM, MANGANESE, IRON, COBALT, NICKEL, COPPER  
YTTRIUM, ZIRCONIUM, NIOBIUM, TUNGSTEN AND BISMUTH

O.A. Salnikov, G.N. Lovchikova, G.V. Kotelnikova,  
A.M. Trufanov, N.I. Fetisov

(Submitted to Bjulleten' CJaD GKAE No. 7(1971))

The paper gives the energy spectra of inelastically scattered neutrons with an initial energy of 14.4 MeV for the case of Cr, Mn, Fe, Co, Ni, Cu, Y, Zr, Nb, W and Bi.

The spectra were obtained for different neutron scattering angles from 30 to 150° with an angular resolution of  $\pm 8^\circ$  and measured by the time-of-flight technique in a cylindrical geometry.

DIFFERENTIAL CROSS-SECTIONS FOR THE INELASTIC SCATTERING OF  
NEUTRONS BY Cr, Mn, Fe, Co, Ni, Cu, Y, Zr, Nb, W  
AND Bi NUCLEI

G.N. Lovchikova, O.A. Salnikov, G.V. Kotelnikova,  
A.M. Trufanov and N.I. Fetisov

(Submitted to Bjulleten' CJaD GKAE<sup>9</sup> No. 7(1971))

The paper presents the differential cross-sections of neutrons with an initial energy of 14.36 MeV inelastically scattered by chromium, manganese, iron, cobalt, nickel, copper, yttrium, zirconium, niobium, tungsten and bismuth nuclei. The measurements were performed by the time-of-flight technique in a cylindrical geometry.

MULTIGROUP CONSTANTS OF THE INELASTIC SCATTERING OF FAST  
NEUTRONS BY IRON, NICKEL, STAINLESS STEEL AND LEAD NUCLEI

V.I. Popov, A.P. Suvorov and L.S. Tarasko

(Paper presented at the French-Soviet Seminar,  
Dubna, 1970)

The parameters of inelastic scattering of fast neutrons by the nuclei of different isotopes of iron, nickel and lead were obtained by the "pseudo-level" method consisting in the interpolation, evaluation and compact representation of inelastic scattering data. The data obtained were used to calculate the multigroup transition matrix due to inelastic scattering for the case of iron, nickel, stainless steel and lead nuclei. A comparison is made with other well-known multigroup constant systems.

INELASTIC NEUTRON SCATTERING -  $(n, n'\gamma)$  - BY FLUORINE,  
IRON, COBALT, NICKEL AND TANTALUM NUCLEI

D.L. Broder, A.F. Gamaly, A.I. Lashuk and I.P. Sadokhin

(Paper presented at the Second International Conference  
on Nuclear Data for Reactors, Helsinki, 1970)

Using a Ge(Li) semiconductor spectrometer the authors measured the cross-sections for the formation of gamma rays in inelastic neutron scattering by various nuclei: fluorine - for gamma lines with energies 110 and 200 keV in the neutron energy range 0.14-3.14 MeV; iron - for gamma lines with energies 847, 1030, 1240, 1250, 1410, 1810, 2100, 2112, 2280, 2350, 2430, 2545, 2610, 2775 and 3210 keV in the neutron energy range 0.90-6.0 MeV; cobalt - for gamma lines with energies 1095, 1190, 1280 and 1400 keV in the neutron energy range 1.14-2.68 MeV; nickel - for gamma lines with energies 1000, 1170, 1332, 1450, 1795, 2150 and 2210 keV in the neutron energy range 1.20-6.0 MeV; tantalum - for gamma lines with energies 137, 153, 302 and 482 keV in the neutron energy range 0.17-2.86 MeV. On the basis of the experimental data and of the energy level schemes of these nuclei conclusions are drawn regarding the excitation of individual levels and the total cross-section for inelastic neutron scattering.



MEASUREMENT OF THE SPECTRA OF PHOTONEUTRONS FROM THE  
 $^{56}\text{Fe}(\gamma, n)^{55}\text{Fe}$  REACTION NEAR THE THRESHOLD

A.I. Abramov, V.Ya. Kitaev, Yu.Ya. Stavitsky and M.G. Yutkin

(Submitted to Jadermaya Fizika)

The paper presents the results of the first spectrum measurements of photoneutrons from the  $^{56}\text{Fe}(\gamma, n)^{55}\text{Fe}$  reaction near the threshold by the time-of-flight technique in the microtron of the Institute of Physics and Power Engineering. The measurements were carried out in the 0.6–25 keV neutron energy range with a resolution of  $\sim 30$  nsec/m at a maximum retardation spectrum energy of  $\sim 12$  MeV. Several peaks were detected in the photoneutron yield in the energy range of up to 10 keV, the position of which, within the limits of experimental error, agrees with the data of other works. The paper discusses the possibilities of using the results of such measurements to obtain data on the cross-sections of the inverse reaction of radiative neutron capture, on the values of partial widths of resonance levels, force functions and so on.

ANALYSIS OF THE VALUES OF  $\bar{\nu}$  ON THE BASIS OF THE ENERGY BALANCE IN  
 $^{233}\text{U}$  AND  $^{239}\text{Pu}$  FISSION BY 0–1.6 MeV NEUTRONS

N.P. Kolosov, B.D. Kuzminov, A.I. Sergachev and V.M. Surin

(Submitted to Jadermaya Fizika)

The energy dependence of  $\bar{\nu}$  in  $^{233}\text{U}$  and  $^{239}\text{Pu}$  fission by neutrons in an energy range of 0–1.6 MeV is obtained from an analysis of the fission energy balance in conjunction with the results of measurements of the yields and kinetic energies of fission fragments and the experimental data on  $\bar{\nu}$  as a whole.

ANALYSIS OF THE NEUTRON ENERGY DEPENDENCE OF  $\bar{\nu}$ , ON THE BASIS  
OF THE ENERGY BALANCE IN NUCLEAR FISSION

V.G. Vorobyeva, P.P. Dyachenko, N.P. Kolosov, B.D. Kuzminov  
A.I. Sergachev, L.D. Smirenkina\*/and A. Lajtai\*\*/

(Paper presented at the Second International Conference of Nuclear Data  
for Reactors, Helsinki, 1970)

The paper analyses the  $E_n$  dependence of  $\bar{\nu}$  on the basis of the energy balance, using the measurements of fission fragment mass and kinetic energy distributions in  $^{232}\text{Th}$ ,  $^{235}\text{U}$  and  $^{238}\text{U}$ , and  $^{239}\text{Pu}$  fission by neutrons with an energy of  $0 \leq E_n \leq 6$  MeV. The table gives the values of  $\alpha$  and  $\bar{\nu}(E_n^0)$  obtained by the method of least squares for  $^{232}\text{Th}$ ,  $^{235}\text{U}$ ,  $^{238}\text{U}$  and  $^{239}\text{Pu}$  nuclei.

Target nucleus	$E_n^0$ MeV	$\bar{\nu}(E_n^0)$	$\alpha$ MeV <sup>-1</sup>
Pu <sup>239</sup>	Thermal	2,898	0,104
U <sup>235</sup>	Thermal	2,418	0,125
U <sup>238</sup>	1,50	2,540	0,140
Th <sup>232</sup>	1,65	2,118	0,175

\*/ Institute of Physics and Power Engineering

\*\*/ Central Physics Research Institute, Hungarian People's Republic

FRAGMENT YIELDS AND KINETIC ENERGIES IN  $^{233}\text{U}$  AND  $^{239}\text{Pu}$   
FISSION BY 5.5 MeV AND 15 MeV NEUTRONS

V.M. Surin, A.I. Sergachev, N.I. Rezhnikov and  
B.D. Kuzminov

(Submitted to Jadernaja Fizika)

Measurements were carried out on the mass and kinetic energy distribution of fragments in  $^{233}\text{U}$  and  $^{239}\text{Pu}$  fission by neutrons with an energy of 5.5 and 15 MeV. It was noted that the yields of the symmetric fragments increased substantially and the average kinetic energy of the fragments decreased. The changes in the kinetic fragments with the different masses are not identical either in absolute value or in sign.

ENERGY DEPENDENCE OF THE YIELDS AND KINETIC ENERGIES OF  
 $^{235}\text{U}$  FISSION FRAGMENTS

P.P. Dyachenko, B.D. Kuzminov, L.S. Kutsaeva and  
V.M. Piksaikin

The paper gives the results of a study of the fragment energy and mass distributions in  $^{235}\text{U}$  fission by monoenergetic neutrons in the 0.6-3 MeV energy range, in steps of 100-250 keV. The results confirm the irregularities noticed previously [1] in the energy dependence of the fragment yields and kinetic energies in the 1.5-2 MeV neutron energy range. A number of difficulties were encountered when the existing models were used to interpret the effects observed.

REFERENCE

- [1] DYACHENKO, P.P., KUZMINOV, B.D., TARASKO, M.Z., Jadernaja Fizika 8 (1968) 286.

THE INFLUENCE OF EXCITATION ENERGY ON THE FRAGMENT YIELDS  
AND KINETIC ENERGIES IN  $^{239}\text{Pu}$  FISSION BY NEUTRONS

N.I. Akimov, V.G. Vorobyeva, V.N. Kabenin, N.P. Kolosov,  
B.D. Kuzminov, A.I. Sergachev, L.D. Smirenkina  
and M.Z. Tarasko

(Submitted to *Jadernaja Fizika*)

A study was made of the mass and kinetic energy distributions of fragments in  $^{239}\text{Pu}$  fission by neutrons with an energy of 0-5.5 MeV, in steps of 100 keV.

It was noted that the average kinetic energy of fragments decreased with increasing excitation energy of the fissionable compound nucleus of  $^{240}\text{Pu}$ .

At neutron energies of 0.6 and 1.1 MeV, the kinetic energy of fragments falls abruptly by approximately 200 keV. In the neutron energy range studied, the fragment yields do not change appreciably.

The effects observed indicate that the transient states of the fissionable nucleus may influence the mass and kinetic energy distributions of the fragments.

ALLOWANCE FOR THE EFFECT OF NEUTRON EMISSION IN THE CASE OF  
FRAGMENT YIELDS OBTAINED BY MEASUREMENT OF FRAGMENT ENERGIES

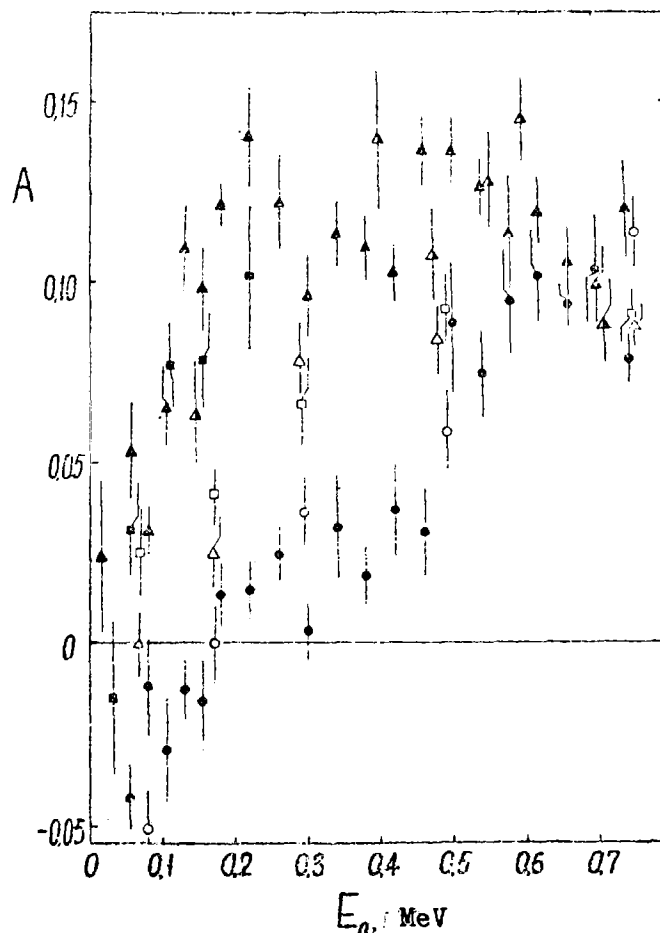
M.Z. Tarasko, L.S. Kutsaeva and P.P. Dyachenko

The paper describes the algorithm and presents the programme written in ALGOL-60 language for obtaining the yields of primary and residual fragments and also the average total kinetic energy of the primary fragments as a function of their masses, on the basis of the measurement of the kinetic energies of additional fragments.

ANGULAR ANISOTROPY AND TARGET NUCLEUS SPIN IN  
THE (n,f) REACTION

G.N. Smirenkin, D.L. Shpak, Yu.B. Ostapenko  
and B.I. Fursov

The angular anisotropy of  $^{233}\text{U}$ ,  $^{235}\text{U}$  and  $^{239}\text{Pu}$  fission was studied extensively as a function of the energy of incident neutrons in the range below 0.7 MeV by the glass method in an electrostatic generator. The experimental data are used to discuss the problem of the effect of the target nucleus spin  $I_0$  on the angular anisotropy of fission  $A$ . A satisfactory qualitative description of the nature of the relationship  $A(E_n, I_0)$  can be obtained by means of the statistical theory of angular distribution of fission fragments.



ANGULAR ANISOTROPY AND NUCLEON PAIRING EFFECTS IN  
 $^{239}\text{Pu}$  FISSION BY NEUTRONS

D.L. Shpak, Yu.B. Ostapenko and G.N. Smirenkin

Glass detectors were used to study the angular anisotropy of  $^{239}\text{Pu}$  (n,f) fission as a function of neutron energy in the 0.05-7.20 MeV range. The pair correlations of nucleons of the superconducting type are shown to have a considerable influence on the spectrum of the transient states of the  $^{240}\text{Pu}$  nucleus. The authors determined the critical energy of phase transition  $E_{cr}^* = 12 \pm 2.5$  MeV and the energy gap  $2\Delta_0^f = 1.7 \pm 0.2$  MeV. A number of inferences are drawn concerning the fission barrier structure.

Table 1. Angular anisotropy A as a function of neutron energy  $E_n$  in  $^{239}\text{Pu}$  fission.

(a) Measurements at angle  $\varphi \approx 150^\circ$

$E_n$ , MeV	A	$E_n$ , MeV	A
0,015 $\pm$ 0,015	0,025 $\pm$ 0,021	0,380 $\pm$ 0,015	0,121 $\pm$ 0,012
0,055 $\pm$ 0,015	0,054 $\pm$ 0,015	0,420 $\pm$ 0,015	0,103 $\pm$ 0,011
0,080 $\pm$ 0,015	0,045 $\pm$ 0,013	0,460 $\pm$ 0,015	0,157 $\pm$ 0,019
0,105 $\pm$ 0,015	0,053 $\pm$ 0,012	0,500 $\pm$ 0,015	0,141 $\pm$ 0,012
0,130 $\pm$ 0,015	0,103 $\pm$ 0,015	0,540 $\pm$ 0,015	0,149 $\pm$ 0,018
0,155 $\pm$ 0,015	0,096 $\pm$ 0,016	0,580 $\pm$ 0,015	0,112 $\pm$ 0,018
0,180 $\pm$ 0,015	0,148 $\pm$ 0,016	0,620 $\pm$ 0,015	0,132 $\pm$ 0,009
0,220 $\pm$ 0,015	0,142 $\pm$ 0,013	0,660 $\pm$ 0,015	0,097 $\pm$ 0,016
0,260 $\pm$ 0,015	0,123 $\pm$ 0,017	0,700 $\pm$ 0,015	0,098 $\pm$ 0,015
0,300 $\pm$ 0,015	0,127 $\pm$ 0,027	0,740 $\pm$ 0,015	0,122 $\pm$ 0,020
0,340 $\pm$ 0,015	0,121 $\pm$ 0,013		

(b) Measurements at angle  $\theta^2 = 12,5^\circ$

$E_n$ , MeV	$A$	$E_n$ , MeV	$A$
0,33 ± 0,05	0,120 ± 0,011	2,40 ± 0,05	0,123 ± 0,010
0,70 ± 0,05	0,099 ± 0,006	2,55 ± 0,05	0,131 ± 0,013
0,80 ± 0,05	0,092 ± 0,012	2,70 ± 0,05	0,126 ± 0,010
0,90 ± 0,05	0,136 ± 0,011	2,85 ± 0,05	0,146 ± 0,011
1,00 ± 0,05	0,120 ± 0,015	3,00 ± 0,05	0,150 ± 0,015
1,10 ± 0,05	0,126 ± 0,015	3,15 ± 0,05	0,138 ± 0,011
1,20 ± 0,05	0,116 ± 0,019	3,30 ± 0,05	0,116 ± 0,010
1,35 ± 0,05	0,114 ± 0,013	3,75 ± 0,05	0,144 ± 0,015
1,50 ± 0,05	0,133 ± 0,014	3,90 ± 0,05	0,125 ± 0,013
1,65 ± 0,05	0,125 ± 0,013	4,05 ± 0,05	0,154 ± 0,012
1,80 ± 0,05	0,138 ± 0,007	4,20 ± 0,05	0,150 ± 0,016
1,95 ± 0,05	0,122 ± 0,014	4,35 ± 0,05	0,146 ± 0,010
2,10 ± 0,05	0,147 ± 0,007	4,50 ± 0,05	0,128 ± 0,013
2,25 ± 0,05	0,114 ± 0,011	4,65 ± 0,05	0,146 ± 0,021
4,80 ± 0,05	0,138 ± 0,011	6,00 ± 0,05	0,171 ± 0,012
4,90 ± 0,05	0,137 ± 0,015	6,15 ± 0,05	0,163 ± 0,014
4,95 ± 0,05	0,147 ± 0,010	6,30 ± 0,05	0,200 ± 0,014
5,10 ± 0,05	0,157 ± 0,012	6,45 ± 0,05	0,207 ± 0,014
5,25 ± 0,05	0,152 ± 0,008	6,60 ± 0,05	0,197 ± 0,019
5,40 ± 0,05	0,129 ± 0,018	6,75 ± 0,05	0,194 ± 0,022
5,55 ± 0,05	0,163 ± 0,019	6,90 ± 0,05	0,206 ± 0,015
5,70 ± 0,05	0,140 ± 0,017	7,05 ± 0,05	0,160 ± 0,012
5,85 ± 0,05	0,176 ± 0,014	7,20 ± 0,05	0,229 ± 0,13

DELAYED NEUTRONS AND THE PHYSICS OF FISSION

B.P. Maksyutenko

(Submitted to Bjulleten' CYaD GKAE No. 7  
(1971))

The analysis of decay curves by the best method in use at present, i.e. the method of least squares, does not give the delayed-neutron yields from pure precursors but from a mixture of precursors, since it is not possible to separate out more than six exponents (their number being much higher) by this method. The meaning of this type of solution is that one obtains the best possible description of the decay curve by some average parameters having no physical content.

A new mathematical method used in analysing the decay curves of the delayed neutrons produced in  $^{235}\text{U}$  fission by thermal neutrons affords a means of separating out a larger number of precursors, some of which consist of pure precursors and the others of a mixture of precursors having identical half-lives, within the experimental errors. From the part consisting of pure precursors one can find the charge distribution in fission, on the basis of which the pure precursors can be separated from the mixed groups as well. Thus, the calculation method developed by us can be used to separate in the pure form the yields of precursors - bromium, rubidium and iodine isotopes accounting for most of the delayed neutron yield, and the problem becomes physically meaningful.

It was found that the distribution of the cumulative mass yields of the fission products - isotopes - can be described by a Gaussian. By using the parameters of this distribution, it is possible to solve the problem of separation of the delayed neutron yields from the pure precursors with even greater accuracy than by using charge distribution.

Some laws governing the behaviour of the probabilities of delayed neutron emission were discovered. Half-lives were studied as a function of mass number and energy of beta decay. On this basis, a review was made of the half-lives and yields of the delayed neutrons of rubidium isotopes and appropriate corrections made in the precursor table prepared from radio-chemical and mass-spectrometric measurement data.

It is shown that the laws discovered and the calculation method based on the measured decay curves of delayed neutrons can be of use in establishing



the charge distributions and the distribution of cumulative fragment yields at  $Z = \text{const}$  in the case of bromium, rubidium and iodine isotopes. The variation of these values with variations in the energy of neutrons responsible for fission is also studied.

### $^{48}\text{V}$ YIELDS IN NUCLEAR REACTIONS IN A CYCLOTRON

P.P. Dmitriev, I.O. Konstantinov and N.N. Krasnov

(Submitted to Atomnaja Energija)

In the cyclotron of the Institute of Physics and Power Engineering the yield of the isotope  $^{48}\text{V}$  was measured as a function of particle energy in the irradiation of thick targets of titanium by protons, deuterons and alpha particles and those of scandium by alpha particles as well as the yield of  $^{48}\text{V}$  in the irradiation of chromium by deuterons with an energy of 20.3 MeV.

The particle energy was varied by means of retarding foils. Stacks of titanium foils were also irradiated. The measurement method is similar to that described by Krasnov and Dmitriev [1]. The data obtained in the work are compared with the measurement results of other authors, and show that irradiation of titanium by protons is the most efficient method of obtaining  $^{48}\text{V}$ .

#### REFERENCE

[1] KRASNOV, N.N., DMITRIEV, P.P., Atomn. Energ. 50 (1966) 57; 21 (1966) 52.

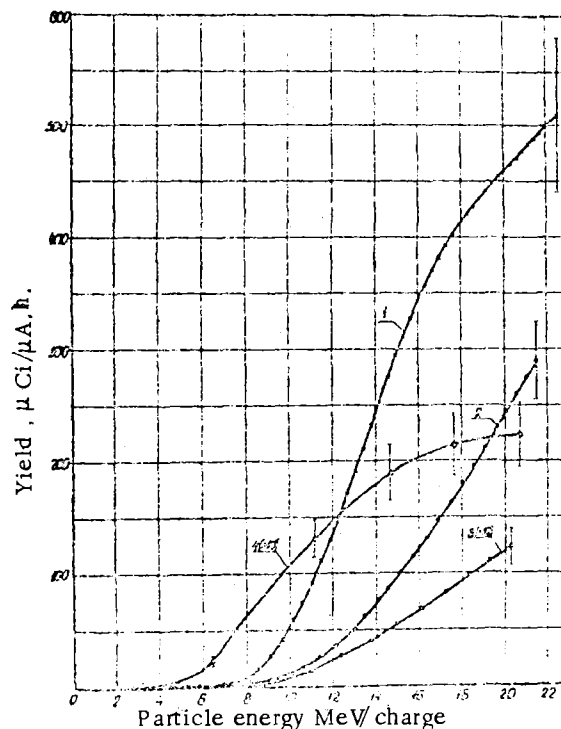


Fig. 1.  $^{48}\text{V}$  yield as a function of particle energy in the irradiation of thick titanium and scandium targets: (1) Ti+p; (2) Ti+d; (3) Ti+ $\alpha$ ; (4) Sc+ $\alpha$ .

Table 1.  $^{48}\text{V}$  yield in the case of thick targets at different energies of incident particles.

Method of obtaining and type of reaction	Particle energy (MeV) and yield ( $\mu\text{Ci}/\mu\text{A.h}$ )										
$\text{Ti} + p$ ( $p,n$ ) ( $p,2n$ )	$E_p$	22,3	20	18	16	14	12	10	8	6	4
	$B$	510	457	41	341	242	135	55	11	-	-
$\text{Ti} + d$ ( $d,n$ ) ( $d,2n$ ) ( $d,3n$ )	$E_d$	21,5	20	18	16	14	12	10	8	6	-
	$B$	290	244	179	123	74	36	13	5	1,5	-
$\text{Ti} + \alpha$ ( $\alpha,pn$ ) ( $\alpha,2n$ ) ( $\alpha p,2n$ ) ( $\alpha,3n$ )	$E_\alpha$	40,6	36	32	28	24	20	16	12	8	-
	$B$	12,3	9,2	6,7	4,4	2,2	0,7	0,2	-	-	-
$\text{Sc} + \alpha$ ( $\alpha,n$ )	$E_\alpha$	41,5	36	32	28	24	20	16	12	8	-
	$B$	22,3	21,5	20,1	18	14,7	10,5	5,9	0,6	-	-
$\text{Cr} + d$ ( $d,\alpha$ ) ( $d,\alpha,2n$ )	$E_d$	20,3	-	-	-	-	-	-	-	-	-
	$B$	2	-	-	-	-	-	-	-	-	-

METHODS OF OBTAINING THE  $^{51}\text{Cr}$  ISOTOPE IN A CYCLOTRON

P.P. Dmitriev, I.O. Konstantinov and N.N. Krasnov

(Submitted to Atomnaja Energija)

In the cyclotron of the Institute of Physics and Power Engineering,  $^{51}\text{Cr}$  yield was measured as a function of particle energy in the irradiation of thick targets of vanadium by protons and deuterons, those of titanium by alpha particles and those of chromium by protons, deuterons and alpha particles. Foil stands were used to measure the excitation functions of the  $^{51}\text{V}(p,n)^{51}\text{Cr}$  and  $^{51}\text{V}(d,2n)^{51}\text{Cr}$  reactions, which are compared with the theoretical cross-sections calculated by the statistical theory. The calculations were performed at values of parameter  $r_0$  in which there is agreement between theory and experiment at the maximum of the excitation function.

The experimental procedure is similar to that described by Dmitriev, Konstantinov and Krasnov [1].

The measurement results are compared with the data of other authors.

REFERENCE

- [1] DMITRIEV, P.P., KONSTANTINOV, I.O., KRASNOV, N.N., Atomn. Energ. 22 (1967) 310.

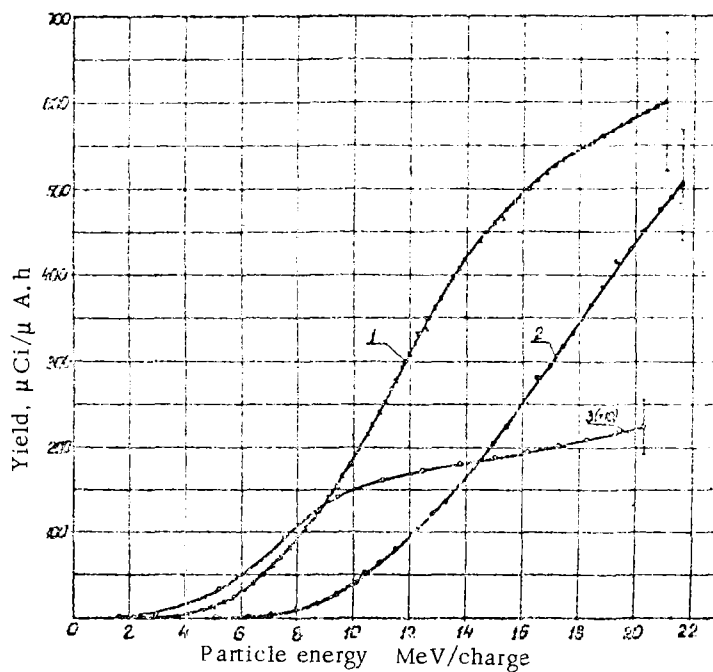


Fig. 1.  $^{51}\text{Cr}$  yield as a function of particle energy in the irradiation of thick targets of vanadium by protons and deuterons and those of titanium by alpha particles: (1) V+p; (2) V+d; (3) Ti+α.

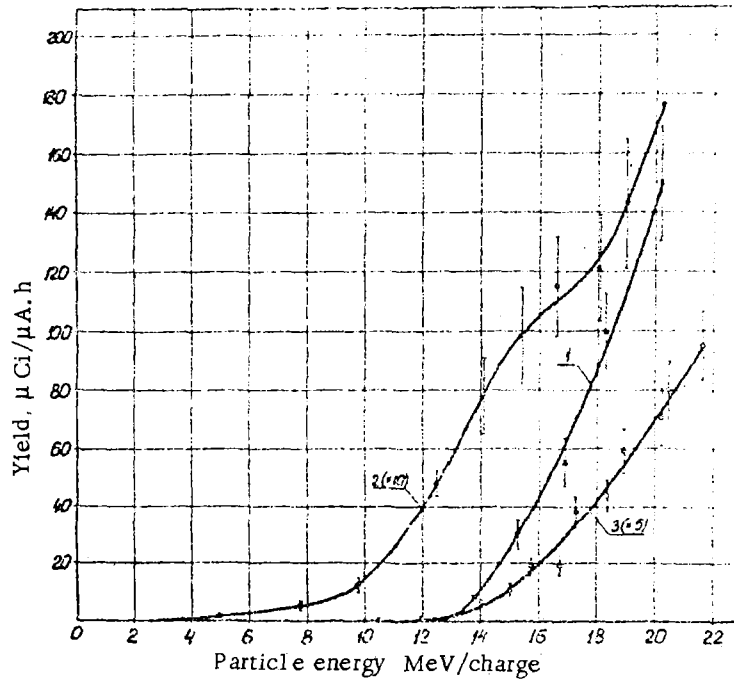


Fig. 2.  $^{51}\text{Cr}$  yield as a function of particle energy in the irradiation of chromium by protons, deuterons and alpha particles: (1) Cr+p; (2) Cr+d; (3) Cr+ $\alpha$ .

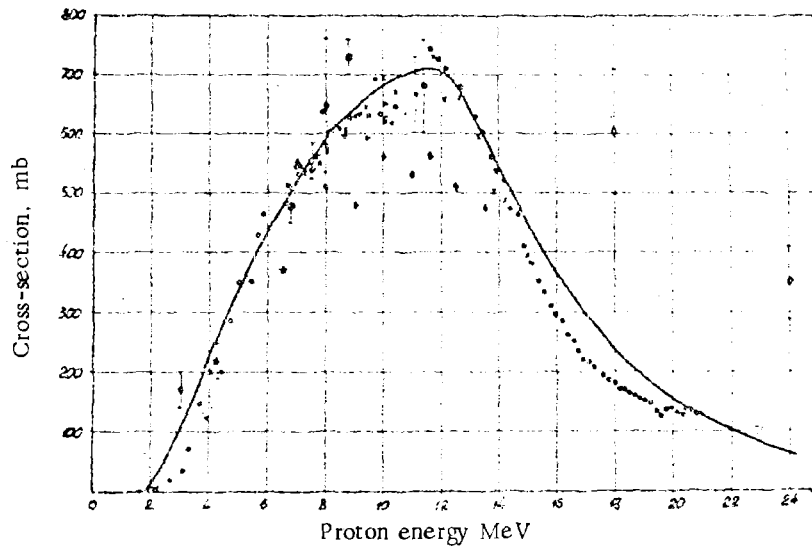


Fig. 3. The excitation function of the  $^{51}\text{V}(p,n)^{51}\text{Cr}$  reaction calculated at  $r_0 = 1.57$  fermi.

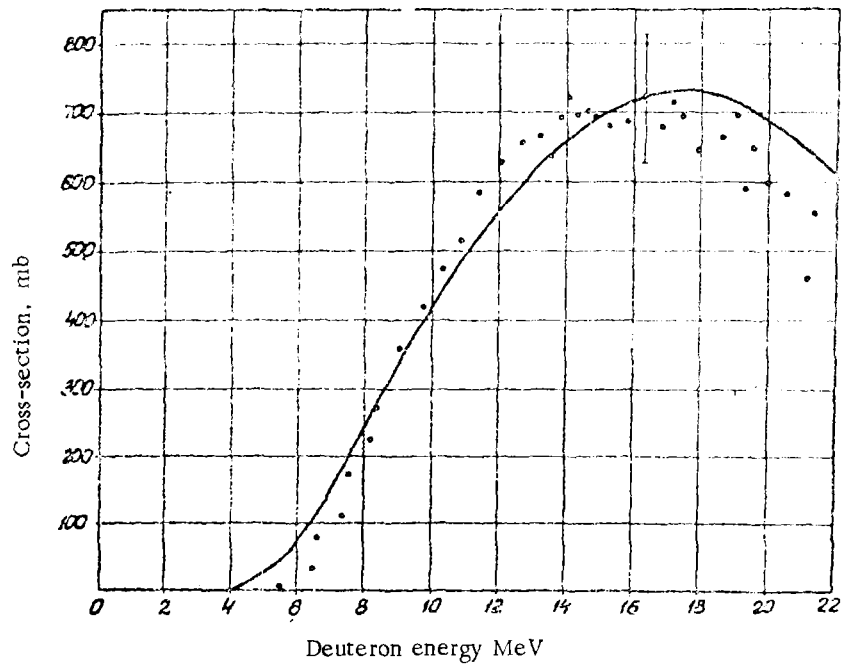


Fig. 4. The excitation function of the  $^{51}\text{V}(d,2n)^{51}\text{Cr}$  reaction calculated at  $r_0 = 1.25$  fermi.

Table 1

<sup>51</sup>Cr yields in the case of thick targets at different incident particle energies.

Method of obtaining and type of reaction	Particle energy (MeV) and yield (μCi/μA.h)									
	21	20	18	16	14	12	10	8	6	4
V + p (pn)	600	582	547	495	424	315	188	91	29	33
V + d (d,2n)	505	443	349	253	167	95	41	9	1	-
Ti + d (dn)(d,2n)(d,3n)	40,6	36	32	28	24	20	16	12	8	4
Cr + p (ppn)(p,2n)	20,2	18	16	14	12	10	8	6	4	2
Cr + d (d,p)(d,n)(dt)(d,dn)	17,6	12,4	10,5	7,7	4	1,4	0,5	0,2	-	-
Cr + α (α,2pn)(α,p,2n)	43,3	40	36	32	28	24	20	16	12	8
Cr + α (α,d,n)(α,d,2n)	19	13,6	8,2	4	0,9	0,2	-	-	-	-

Table 2

Experimental cross-sections of nuclear reactions

$V^{51}(p, n)Cr^{51}$					
E, MeV	σ, mb	E, MeV	σ, mb	E, MeV	σ, mb
2,70±0,80	20 ± 3	11,89 ± 0,64	727 ± 95	17,32 ± 0,52	208 ± 26
3,33±0,79	70 ± 10	12,15 ± 0,63	710 ± 94	17,51 ± 0,52	194 ± 24
3,92±0,78	122 ± 17	12,70 ± 0,62	676 ± 86	17,70 ± 0,51	187 ± 23
4,43±0,78	202 ± 28	13,20 ± 0,61	630 ± 84	17,91 ± 0,51	182 ± 22
4,94±0,77	209 ± 29	13,44 ± 0,61	604 ± 81	18,11 ± 0,51	172 ± 21
5,40±0,76	351 ± 47	13,72 ± 0,60	551 ± 76	18,30 ± 0,50	171 ± 21
5,80±0,75	418 ± 57	13,97 ± 0,60	539 ± 74	18,49 ± 0,50	166 ± 20
6,67±0,75	482 ± 65	14,20 ± 0,59	521 ± 71	18,64 ± 0,50	161 ± 20
7,09±0,74	545 ± 74	14,40 ± 0,58	470 ± 62	18,82 ± 0,49	154 ± 19
7,49±0,73	540 ± 73	14,62 ± 0,58	465 ± 60	19,02 ± 0,49	150 ± 19
7,84±0,73	637 ± 85	14,85 ± 0,57	412 ± 54	19,21 ± 0,49	149 ± 18
8,18±0,72	601 ± 82	15,10 ± 0,57	388 ± 52	19,40 ± 0,48	130 ± 16
8,50±0,72	608 ± 82	15,37 ± 0,56	355 ± 47	19,58 ± 0,48	126 ± 16
8,82±0,71	626 ± 85	15,59 ± 0,56	335 ± 44	19,73 ± 0,47	125 ± 16
9,15±0,70	634 ± 85	15,79 ± 0,55	316 ± 40	19,90 ± 0,47	123 ± 17
9,45±0,70	593 ± 81	15,98 ± 0,55	296 ± 39	20,11 ± 0,47	122 ± 16

Table 2 continued

I		2		3	
9,74±0,69	694±90	16,15±0,54	286±36	20,30±0,47	129±15
10,02±0,68	620±80	16,33±0,54	266±34	20,43±0,46	134±16
10,30±0,67	618±79	16,53±0,53	253±32	20,58±0,46	131±16
11,15±0,66	668±85	16,74±0,53	237±30	20,76±0,46	129±16
11,40±0,65	762±100	16,94±0,53	221±28	20,95±0,45	129±16
11,65±0,64	744±97	17,13±0,52	218±27		

$V^{51}(d, 2n)Cr^{51}$			
E, MeV	$\sigma$ , mb	E, MeV	$\sigma$ , mb
5,50±0,75	5,0± 0,7	14,30±0,59	698±91
6,50±0,75	32± 5	14,64±0,58	701±91
6,65±0,75	78± II	14,85±0,57	693±90
7,40±0,73	III± 15	15,28±0,56	680±88
7,55±0,73	I70± 22	15,81±0,55	696±89
8,20±0,72	223± 29	16,32±0,54	723±94
8,38±0,72	270±35	16,83±0,53	678±88
9,05±0,70	358± 47	17,15±0,52	713±93
9,71±0,69	418± 55	17,48±0,52	693±90
10,30±0,68	472± 61	17,97±0,51	643±84
10,83±0,67	514± 67	18,62±0,50	662±86
11,40±0,65	584± 76	19,05±0,49	696±90
12,05±0,63	628± 82	19,30±0,48	589±76
12,65±0,62	656±86	19,55±0,48	648±84
13,15±0,61	663± 86	19,97±0,47	597±78
13,53±0,61	633± 82	20,53±0,46	581±76
13,80±0,60	692± 90	21,15±0,45	460±60
14,04±0,60	720± 94	21,38±0,45	555±72

JOINT INSTITUTE OF NUCLEAR RESEARCH (JINR)

PARAMETERS OF NEUTRON RESONANCES OF  $^{233}\text{U}$ ,  $^{235}\text{U}$  AND  $^{239}\text{Pu}$

Yu.V. Ryabov, So Don Sik, N. Chikov and N. Yaneva

(JINR Preprint R3-4992, 1970)

The measurements were performed by the time-of-flight method with the JINR pulsed fast reactor as the resonance neutron source. The flight path  $L$  was 1010 m. The time spectra were recorded by a 4096-channel analyser with channel widths of 8 and 16  $\mu\text{sec}$ . This gave a resolution of  $\frac{\Delta t}{L} \approx (40 \text{ to } 55) \frac{\text{nsec}}{\text{m}}$ . The fission and radiative-capture events were recorded by means of a cylindrical liquid scintillation detector with a capacity of 500 litres; it had a toluene base and contained paraterphenyl, POPOP and cadmium propionate as additives. A boron-containing liquid scintillation detector was used in transmission measurements. The total cross-sections were also measured by the method of self-indication, for which the detector separating channel having a low background level was used.

All the data obtained in the fission, radiative-capture self-indication and transmission measurements were transmitted by cable to the computer for processing. For finding the level parameters  $g\Gamma_n$ ,  $\Gamma_f$ ,  $\Gamma_c$  and  $\Gamma$  by the area method, a system of least-square-method equations was solved on the computer. The processing programme introduced corrections for the resonance tails on the assumption that the cross-sections near the resonance are described by the Breit-Wigner formula for a single level without allowance for interference effects. The use of different types of measurement systematically reduces errors, since the sources of error are different. Moreover, for each type of experiment, the measurements were carried out with several samples, so that a much larger number of equations could be used than the number of unknown parameters. This factor, too, improves the reliability of the results.



Table 1. Characteristics of the  $^{233}\text{U}$ ,  $^{235}\text{U}$  and  $^{239}\text{Pu}$  samples used

Isotope	Type of measurement	Fission, radiative capture	Transmission	Self-indication
Uranium-233 (sample thickness nuclei/barn)			$2,5 \cdot 10^{-4}$ $4,9 \cdot 10^{-4}$ $7,1 \cdot 10^{-4}$ $9,7 \cdot 10^{-4}$	
Uranium-235 (sample thickness nuclei/barn)		$8,31 \cdot 10^{-5}$ $4,27 \cdot 10^{-4}$ $2,14 \cdot 10^{-3}$ $1,30 \cdot 10^{-2}$ $2,20 \cdot 10^{-2}$	$4,27 \cdot 10^{-4}$ $2,14 \cdot 10^{-3}$ $1,30 \cdot 10^{-2}$ $2,20 \cdot 10^{-2}$	$n_D = 2,14 \cdot 10^{-5}$ $n_T = 2,27 \cdot 10^{-3}$ $n_P = 4,27 \cdot 10^{-4}$
Plutonium-239 (sample thickness nuclei/barn)		$2,85 \cdot 10^{-4}$ $5,88 \cdot 10^{-4}$ $8,8 \cdot 10^{-4}$ $1,28 \cdot 10^{-3}$ $2,70 \cdot 10^{-3}$	$2,85 \cdot 10^{-4}$ $5,88 \cdot 10^{-4}$ $1,28 \cdot 10^{-3}$ $2,70 \cdot 10^{-3}$	$n_D = 1,28 \cdot 10^{-5}$ $n_T = 2,85 \cdot 10^{-4}$ $n_P = 5,88 \cdot 10^{-4}$ $n_T = 1,42 \cdot 10^{-3}$

Table 2. Resonance parameters of  $^{234}\text{U}$  and  $^{238}\text{U}$

Isotope	Uranium-234 ( $E_0 = 5,19 \text{ eV}$ )	Uranium -238 ( $E_0 = 6,68 \text{ eV}$ )
Parameters	$\Gamma = 29 \pm 6 \text{ MeV}$	$\Gamma = 27,5 \pm 2,0 \text{ MeV}$
<i>BNL-325</i>	$\Gamma_n = 4,1 \pm 0,5 \text{ MeV}$	$\Gamma_n = 1,52 \pm 0,02 \text{ MeV}$
<i>Suppl N2</i>	$\Gamma_c = 25 \pm 6 \text{ MeV}$	$\Gamma_c = 26 \pm 2 \text{ MeV}$
Present work	$\Gamma = 29,4 \pm 4,7 \text{ MeV}$	$\Gamma = 27,5 \pm 2,3 \text{ MeV}$
	$\Gamma_n = 3,88 \pm 0,35 \text{ MeV}$	$\Gamma_n = 1,49 \pm 0,03 \text{ MeV}$
	$\Gamma_c = 25,5 \pm 4,7 \text{ MeV}$	$\Gamma_c = 26,0 \pm 2,3 \text{ MeV}$

Table 3. Parameters of uranium-235 levels

$E_i$ , eV	$\Gamma_0 \Gamma_f$ b	$\Gamma_0 \Gamma_c$ a	$\Gamma_r$ r	$\Gamma_n$ n	$\Gamma_x$ x	$\Gamma_0(\Gamma_f + \Gamma_c)$ eV	$2g \Gamma_n$	$\Gamma$ m	$\Gamma_f$ e	$\Gamma_c$ v	$d$
0,290 <sup>±0,010</sup>							0,0032 <sup>±0,0005</sup>	135 <sup>±8</sup>	100 <sup>±8</sup>	35 ± 3	0,35
1,135 <sup>±0,010</sup>							0,0154 <sup>±0,0011</sup>	157 <sup>±11</sup>	115 <sup>±10</sup>	42 ± 5	0,37
2,026 <sup>±0,004</sup>	1,47 <sup>±0,05</sup>	4,1 <sup>±0,6</sup>	4,94 <sup>±0,49</sup>	5,57 <sup>±0,60</sup>			0,0077 <sup>±0,0008</sup>	57 <sup>±14</sup>	15 ± 5	42 ± 5	2,8 ± 0,3
2,84 <sup>±0,02</sup>	1,15 <sup>±0,03</sup>	0,35 <sup>±0,14</sup>		1,5 <sup>±0,3</sup>			0,0033 <sup>±0,0007</sup>	186 <sup>±48</sup>	143 <sup>±46</sup>	43 ± 2	0,3 ± 0,1
3,136 <sup>±0,006</sup>	7,9 ± 0,6	2,6 ± 0,4	12,27 <sup>±0,54</sup>	10,5 <sup>±0,8</sup>			0,0296 <sup>±0,0013</sup>	129 <sup>±17</sup>	97 <sup>±18</sup>	32 ± 10	0,33 <sup>±0,08</sup>
3,584 <sup>±0,006</sup>	10,3 <sup>±0,5</sup>	6,4 ± 0,7	19,01 <sup>±0,65</sup>	16,7 <sup>±0,9</sup>			0,0524 <sup>±0,0018</sup>	80 <sup>±7</sup>	49 <sup>±7</sup>	31 ± 6	0,62 <sup>±0,09</sup>
4,81 <sup>±0,01</sup>	2,6 <sup>±0,2</sup>	16,8 <sup>±0,9</sup>	16,7 ± 0,7	19,4 <sup>±0,9</sup>			0,0616 <sup>±0,0026</sup>	29,8 <sup>±6,5</sup>	3,9 <sup>±1,0</sup>	25,9 <sup>±3,6</sup>	6,5 ± 0,9
5,45	2,1 <sup>±0,3</sup>	4,0 <sup>±1,3</sup>	4,8 ± 0,9	6,1 <sup>±1,4</sup>			0,023 ± 0,003	70 <sup>±20</sup>	24 <sup>±7</sup>	46 ± 16	1,9 ± 0,4
5,82	1,6 <sup>±0,5</sup>	1,0 <sup>±0,7</sup>		2,6 <sup>±0,9</sup>			0,012 ± 0,004	110 <sup>±35</sup>	67 <sup>±34</sup>	43 ± 2	0,64 <sup>±0,30</sup>
6,20 ± 0,01	4 <sup>±1</sup>	2,2 <sup>±0,8</sup>	6,3 ± 1,2	6,2 <sup>±1,3</sup>			0,0290 <sup>±0,0055</sup>	132 <sup>±24</sup>	85 <sup>±24</sup>	47 ± 17	0,55 <sup>±0,15</sup>
6,40 ± 0,01	11,5 ± 0,4	53 <sup>±5</sup>	47,1 <sup>±3,3</sup>	65 <sup>±6</sup>			0,232 ± 0,016	63 <sup>±11</sup>	11 <sup>±3</sup>	52 ± 30	4,6 ± 0,6
7,095 ± 0,015	9,1 ± 0,4	13 <sup>±1</sup>	20,5 <sup>±0,7</sup>	22,1 <sup>±1,0</sup>			0,1116 <sup>±0,0036</sup>	53 <sup>±4</sup>	22 <sup>±4</sup>	31 ± 6	1,4 ± 0,2
8,77 ± 0,02	106 ± 4	58 <sup>±5</sup>	182,0 <sup>±5,3</sup>	164 ± 6			1,228 ± 0,036	118 <sup>±10</sup>	76 <sup>±10</sup>	42 ± 7	0,55 <sup>±0,07</sup>
9,30 ± 0,03	13,1 ± 0,5	6,8 ± 0,9	18,3 ± 0,8	20 ± 1			0,131 ± 0,006	172 <sup>±56</sup>	115 <sup>±44</sup>	57 ± 20	0,50 <sup>±0,09</sup>
9,73 ± 0,08	4,3 ± 1,0	2 ± 1		6,3 <sup>±1,4</sup>			0,047 ± 0,015	157 <sup>±60</sup>	94 <sup>±60</sup>	43 ± 2	0,46 <sup>±0,27</sup>
10,20 ± 0,03	4,6 ± 0,6	4,0 ± 0,8	8,4 ± 0,8	8,6 <sup>±1,0</sup>			0,066 ± 0,006	83 <sup>±13</sup>	47 <sup>±14</sup>	40 ± 9	0,87 <sup>±0,13</sup>
10,65 ± 0,06	2	1		3			0,025	129	86	43 ± 2	0,5
11,05	1	2		3			0,026	65	22	43 ± 2	2
11,66 ± 0,04	10,3 ± 0,3	63 ± 5	67,6 ± 2,7	73 ± 5			0,606 ± 0,024	66 <sup>±7</sup>	9 <sup>±1</sup>	57 ± 7	6,20 <sup>±0,67</sup>
12,39 ± 0,04	47 ± 2	85 ± 5	124,9 <sup>±3,7</sup>	132 ± 5			1,190 ± 0,035	66 <sup>±6</sup>	24 <sup>±4</sup>	42 ± 5	1,8 ± 0,2
12,82 ± 0,04	3,1 ± 0,4	1,9 ± 0,6	3,8 ± 0,6	5,0 ± 0,8			0,037 ± 0,006	85 <sup>±23</sup>	52 <sup>±19</sup>	33 ± 14	0,63 <sup>±0,16</sup>
13,28 ± 0,05	3,0 ± 0,5	2,6 ± 0,8	5,3 ± 0,6	5,6 ± 0,9			0,054 ± 0,006	122 <sup>±24</sup>	65 <sup>±20</sup>	57 ± 19	0,87 <sup>±0,22</sup>
13,67 ± 0,10	3,7 ± 1,5	1,5 ± 0,8		5,2 ± 2,1			0,059 ± 0,023	145 <sup>±41</sup>	102 <sup>±41</sup>	43 ± 2	0,42 <sup>±0,15</sup>
13,98 ± 0,05	30 ± 7	7 ± 3		37 ± 8			0,40 ± 0,09	230 <sup>±96</sup>	187 <sup>±98</sup>	43 ± 2	0,25 <sup>±0,11</sup>
14,50 ± 0,05	7,3 ± 1,9	8,7 ± 2,7	9,7 ± 1,3	16 ± 3			0,108 ± 0,014	62 <sup>±10</sup>	28 <sup>±7</sup>	34 ± 8	1,2 ± 0,2

Table 3 (continued)

$E_L$ eV	$G_0 \Gamma_f$ b	$G_0 \Gamma_c$ a r	$G_0 \Gamma'$ n x	$G_0(\Gamma_f \Gamma_c)$ eV	$2g/h$ m	$\Gamma$ e	$\Gamma_f$ V	$\Gamma_c$	$\alpha$
13,40±0,05	10,4±0,4	12±1	19,9±0,8	22±1	0,236±0,010	99±17	47±10	52±11	1,1±0,1
14,50±0,05	9,6±0,3	20±2	28,1±1,1	29,6±2,0	0,348±0,014	44±10	14±4	30±8	2,1±0,2
16,00±0,06	13,7±0,6	9±1	21,7±0,8	22,7±1,2	0,278±0,013	93±19	55±15	38±11	0,7±0,1
16,9±0,1	1	3		4	0,05	57	14	43±2	3
18,05±0,05	17,3±0,7	9±2	27,2±1,6	26,3±2,1	0,378±0,022	141±23	94±21	47±14	0,5±0,1
18,6±0,1	3	2		5	0,07	115	72	43±2	0,6
19,30±0,05	112±4	90±10	223,0±7,8	202±11	3,310±0,116	104±6	58±7	46±6	0,6±0,1
23,10±0,03	3,5±1,3	2,5±1,4		6,0±1,9	0,09±0,03	104±29	61±29	43±2	0,7±0,3
20,62±0,06	5,8±0,8	10,4±2,2		16,2±2,3	0,25±0,04	67±6	24±5	43±2	1,8±0,3
21,13±0,05	33±1	53±10	87,2±5,5	86±10	1,418±0,090	82±16	32±10	50±9	1,6±0,3
21,8±0,1				1	0,02	186	143	43±2	0,3
22,4±0,1				1	0,02	186	143	43±2	0,3
22,90±0,06	13,0±0,3	16±3	24,2±1,8	29±3	0,428±0,031	77±18	35±11	42±13	1,2±0,2
23,43±0,15	4,5±0,9	26±8		30,5±8,1	0,55±0,14	50±3	7±2	43±2	5,8±1,4
23,60±0,07	30±7	19±5	50,7±9,3	49±9	0,924±0,169	111±32	68±24	43±17	0,63±0,11
24,25±0,07	7,5±3,0	10±5	17,9±3,0	17,5±5,8	0,334±0,056	91±28	39±20	52±24	1,53±0,45
24,41±0,15	3,9±1,5	3,9±1,9		7,8±2,4	0,14±0,04	86±15	43±15	43±2	1,0±0,3
25,16±0,16	7,4±2,5	4,1±1,8		11,5±3,1	0,22±0,06	121±25	78±24	43±2	0,55±0,15
25,56±0,10	11±4	20±9	31,9±9,5	31±10	0,628±0,188	74±38	26±18	48±29	1,8±0,5
25,80±0,15	3,0±1,5	2,4±1,5		5,4±2,1	0,11±0,04	97±23	54±22	43±2	0,8±0,3
26,55±0,07	15±3	6,2±2,0	21,8±3,7	21,2±3,6	0,446±0,076	129±48	92±41	37±20	0,4±0,1
27,18±0,07	5,9±1,6	4,6±2,1		8,5±2,6	0,18±0,06	79±11	36±10	43±2	1,2±0,3
27,86±0,07	18±2	8±2	26,6±3,1	26±3	0,570±0,066	96±22	66±20	30±12	0,45±0,10
28,45±0,09	4,6±1,0	3,2±1,2		7,8±1,5	0,17±0,03	104±20	61±20	43±2	0,7±0,2
28,82±0,03	2,0±0,7	2,7±1,3		4,7±1,5	0,10±0,03	74±13	31±12	43±2	1,4±0,5
29,60±0,03	3,0±0,6	5,3±1,4		8,3±1,5	0,19±0,03	67±6	24±5	43±2	1,8±0,3
30,55±0,20	4,1±0,9	5,4±2,0		9,5±2,2	0,22±0,05	76±12	33±12	43±2	1,3±0,4

Table 3 (continued)

$E_i$ eV	$G_0 I_f$ b	$G_0 I_c$ a r n	$G_0 I$ eV	$G_0(I_f + I_c)$	$2g I_n$	$I_m$	$I_f$ e V	$I_c$	$\alpha$
30,86±0,10	6,8±1,5	8,6±3,4		16,4±3,7	0,40±0,09	74±10	31±10	43±2	1,4±0,4
32,10±0,09	38±5	42±6	74,1±6,5	80 ±8	1,83±0,16	120±12	57±10	63±10	1,10±0,15
33,58±0,09	26±5	41±6	72,0±7,7	67 ±8	1,86±0,20	58±7	22±5	36±7	1,6±0,3
34,45±0,14	32±5	48±12		80±13	2,12±0,34	72±7	29±7	43±2	1,5±0,3
34,9 ±0,2	13±4	21±9		34±10	0,9 ±0,3	70±10	27±9	43±2	1,6±0,5
35,27±0,10	107±20	58±17		165±26	4,76±0,54	183±36	119±31	64±20	0,54±0,10
38,40±0,11	13±4	9±4		22±6	0,66±0,18	104±20	61±20	43±2	0,7±0,2
39,47±0,11	39±6	47±11	91,6±11,9	86±13	2,78±0,36	98±11	45±9	53±10	1,2±0,2
39,9 ±0,2	8±3	5,0±2,5		13±4	0,40±0,12	115±27	72±27	43±2	0,6±0,2
40,50±0,15	12±4	5±3		17±5	0,53±0,16	151±56	108±45	43±2	0,40±0,15
41,3 ±0,2	7±3	9±4		16±5	0,51±0,16	76±10	33±10	43±2	1,32±0,35
41,5 ±0,2	4,0±1,5	3,0±1,7		7,0±2,3	0,22±0,07	108±29	65±28	43±2	0,66±0,26
41,8 ±0,2	17±5	22±8		39±10	1,3 ±0,3	76±9	33±9	43±2	1,3 ±0,3
42,2 ±0,3	4,0±1,7	3,0±1,7		7,0±2,4	0,23±0,08	100±26	57±25	43±2	0,75±0,30
42,7 ±0,3	2,0±0,8	2,8±1,4		4,8±1,6	0,15±0,05	74±11	31±10	43±2	1,4 ±0,4
43,4 ±0,2	6±2	6,6±2,5		12,6±3,3	0,42±0,11	72±9	29±9	43±2	1,5 ±0,4
43,9 ±0,2	9±3	7±3		16±4	0,54±0,13	79±11	36±11	43±2	1,2 ±0,3
44,6 ±0,2	12±5	4±2		16±6	0,55±0,21	123±41	80±41	43±2	0,54±0,25
45,0 ±0,3	6,0±2,5	2,2±1,5		8,2±3,0	0,30±0,11	151±59	108±59	43±2	0,4 ±0,2
45,8 ±0,2	5±2	8,5±4,2		13,5±4,5	0,48±0,16	68±9	25±8	43±2	1,7 ±0,5
47,06±0,14	23±5	27±7		50±8	1,8 ±0,3	79±9	36±8	43±2	1,2± 0,2
48,00±0,15	10±3	16±6		26±7	1,0 ±0,3	70±8	27±8	43±2	1,6± 0,4
48,3 ±0,2	12±5	10±6		22±8	0,8 ±0,3	97±23	54±23	43±2	0,8± 0,3
48,6 ±0,2	6,0±2,5	3,0 ±1,7		9±3	0,3 ±0,1	129±38	86±38	43±2	0,5± 0,2
49,3 ±0,3	7 ±2	13±5		20±6	0,8 ±0,2	67±7	24±6	43±2	1,8± 0,4
50,2 ±0,3	4,0±1,5	6±3		10±3	0,4 ±0,1	70±8	27±8	43±2	1,6± 0,4

Table 4. Parameters of plutonium-239 levels

$E_i$ eV	$\Gamma_f/\Gamma$	$2g/\Gamma$ meV	$\Gamma$ meV	$\Gamma_f$ meV	$\Gamma_c$ meV
0,296 <sup>±</sup>	0,61±0,01	0,108±0,004	102±11	62±2	40 ± 10
7,83±0,01	0,526±0,015	1,23 ±0,03	87±6	46±4	39,8±4,0
10,97±0,02	0,776±0,042	2,69 ±0,12	189±19	147±23	39,3±6,0
11,5	0,73	0,41		110	41
11,91±0,02	0,41±0,03	1,43±0,08	68±7	28±5	38,6±7,0
14,36±0,02	0,59±0,05	0,88±0,05	101±8	60±10	40,1±7,0
14,75±0,03	0,43±0,03	2,44±0,10	81±8	35±6	43,6±7,0
15,47±0,06	0,95±0,08	0,87±0,06	761±52	723±110	37,1±6
17,69±0,03	0,50±0,03	2,58±0,04	92±7	47±6	43,4±6
22,33±0,04	0,57±0,03	3,14±0,06	120±10	68±9	48,4±7
23,9 ±0,1	0,37±0,08	0,12±0,02	67±12	25±10	42,0±17
26,31±0,06	0,58±0,04	2,25±0,11	81±9	47±8	31,8±6
27,3	0,32±0,14	0,14±0,10	41±10	13±8	27,9±12
32,4 ±0,1	0,68±0,06	0,42±0,02	141±15	96±18	44,7±9
35,6	0,13±0,03	0,48±0,08	52±11	7±3	44,5±11
41,68±0,12	0,200±0,015	5,93±0,33	78±13	16±4	56,1±10,5
44,60±0,12	0,162±0,015	7,63±0,29	52±8	8±2	36,4±12
47,92±0,15	0,89±0,06	3,01±0,17	273±39	243±51	26,7±6
49,6	0,91	1,3		460	41
50,18±0,16	0,38±0,03	4,35±0,25	77±8	29±5	43,7±7
52,8 ±0,2	0,16±0,02	12,4±0,4	63±9	10±3	40,6±7
55,9 ±0,4	0,43±0,03	2,43±0,21	67±10	29±6	35,6±8
57,8 ±0,2	0,86±0,05	9,37±0,41	467 ±116	402±123	55,6±17
58,6 ±0,4	0,94±0,06	3,91±0,48	760 ±222	714±254	42,1±15
59,6 ±0,2	0,72±0,03	12,8±1,4	187 ±20	135±20	39,2±6
61,7 ±0,2	0,76±0,05	1,46±0,31	210 ±39	160±40	48,5±12

Table 4 (continued)

$E_i$ eV	$\Gamma_i/r$	$2g\Gamma_n$ meV	$\Gamma$ meV	$\Gamma_f$ meV	$\Gamma_c$ meV
$63,4 \pm 0,2$	$0,69 \pm 0,04$	$8,4 \pm 0,6$	$156 \pm 21$	$108 \pm 21$	$39,6 \pm 8$
$66,2 \pm 0,2$	$0,62 \pm 0,04$	$18,36 \pm 0,87$	$136 \pm 18$	$84 \pm 17$	$33,7 \pm 7$
69,9	0,48	2,9		40	41
$75,6 \pm 0,3$	$0,53 \pm 0,05$	$36,6 \pm 1,8$	$154 \pm 19$	$82 \pm 18$	$35,4 \pm 8$
$82,7 \pm 0,3$	$0,58 \pm 0,07$	$6,8 \pm 0,9$	$124 \pm 36$	$72 \pm 30$	$45,2 \pm 19$
$85,7 \pm 0,4$	$0,91 \pm 0,07$	$38,7 \pm 5,4$	$881 \pm 249$	$802 \pm 288$	$40,3 \pm 15$

Table 5

Parameters of uranium-233

$E_i$ eV	$2g\Gamma_n$ meV	$\Gamma$ meV
$1,79 \pm 0,01$	$0,35 \pm 0,04$	$330 \pm 50$
$2,32 \pm 0,02$	$0,17 \pm 0,04$	$60 \pm 20$
$3,68 \pm 0,02$	$0,13 \pm 0,02$	$220 \pm 40$
$4,82 \pm 0,03$	$0,25 \pm 0,07$	$600 \pm 280$
$6,85 \pm 0,04$	$0,61 \pm 0,12$	$170 \pm 60$
$10,50 \pm 0,06$	$1,5 \pm 0,3$	$270 \pm 90$
$12,85 \pm 0,08$	$1,3 \pm 0,4$	$340 \pm 120$
$13,9 \pm 0,1$	$0,33 \pm 0,07$	$380 \pm 130$
$15,5 \pm 0,1$	$0,84 \pm 0,34$	$200 \pm 60$
$16,6 \pm 0,2$	$1,16 \pm 0,25$	$650 \pm 130$
$18,2 \pm 0,2$	$0,26 \pm 0,09$	$200 \pm 50$
$19,0 \pm 0,2$	$1,6 \pm 0,3$	$300 \pm 130$
$20,6 \pm 0,2$	$1,3 \pm 0,2$	$450 \pm 110$

Table 6. Evaluations of the average characteristics of levels of uranium-235 and plutonium-239 for two spin states of the compound nucleus

Nucleus	J	$\langle \Gamma_n^0 \rangle^J$ MeV	$\langle \Gamma_f \rangle^J$ MeV	$\langle \Gamma_{eff} \rangle^J$	$\langle \Gamma_c \rangle^J$ MeV	$\langle D \rangle^J$ eV	$S_0^J \cdot 10^{-4}$
U - 235	3 <sup>-</sup>	0,102 ± 0,023	87 ± 20	0,42	42 ± 2	1,26 ± 0,10	0,71 <sup>+0,32</sup> <sub>-0,17</sub>
	4 <sup>-</sup>	0,115 ± 0,025	26 ± 6	0,13	43 ± 2	1,26 ± 0,10	0,81 <sup>+0,36</sup> <sub>-0,19</sub>
Pu - 239	0 <sup>+</sup>	0,51 ± 0,21	290 ± 100	0,19	45 ± 3	8,26 ± 1,14	0,60 <sup>+0,44</sup> <sub>-0,18</sub>
	1 <sup>+</sup>	0,49 ± 0,15	45 ± 15	0,088	43 ± 2	3,78 ± 0,44	1,22 <sup>+0,71</sup> <sub>-0,31</sub>

Table 7. Coefficients of correlation between the resonance parameters of uranium-235 and plutonium-239

U - 235	$\rho(2\sigma \Gamma_n^0, \Gamma_f)$	= - 0,04 ± 0,18
	$\rho(2\sigma \Gamma_n^0, \Gamma_c)$	= - 0,40 ± 0,34
	$\rho(\Gamma_f, \Gamma_c)$	= - 0,11 ± 0,26
Pu - 239	$\rho(\Gamma_n^0, \Gamma_f)$	= 0,30 ± 0,29
	$\rho(\Gamma_n^0, \Gamma_c)$	= - 0,09 ± 0,51
	$\rho(\Gamma_f, \Gamma_c)$	= 0,03 ± 0,61

MEASUREMENTS OF THE RATIOS OF RADIATIVE-CAPTURE AND FISSION ( $\alpha$ )  
CROSS-SECTIONS FOR  $^{235}\text{U}$  AND  $^{239}\text{Pu}$  IN THE NEUTRON ENERGY  
RANGE BELOW 30 keV

M.A. Kurov, Yu.V. Ryabov, So Don Sik and N. Chikov  
(JINR Preprint R3-5112, 1970)

Measurements of  $\alpha(E) = \sigma_c(E)/\sigma_f(E)$  for  $^{235}\text{U}$  and  $^{239}\text{Pu}$  were performed with the JINR time-of-flight neutron spectrometer in an effort to refine the results published earlier in *Atomn. Energ.* 24 (1968) 351. The measurement procedure has been described earlier. The measurements of the time dependence of the fission and radiative-capture count rates for small time lags in relation to the neutron pulse of the reactor impose strict requirements in respect of background counting accuracy. A reduction in the variable component of the background in an operating reactor, in comparison with the first measurements (1968), was achieved by the following procedures:

- (a) The neutron beam was shaped with collimators and filters outside the experimental area. This led, in the building, to a substantial reduction in the scattering of fast neutrons on collimators, structural materials of the detector and so on;
- (b) A vacuum channel was built inside the detector, eliminating the contribution of neutron scattering in air;
- (c)  $^{10}\text{B}$  and  $^6\text{Li}$  filters were used with paraffin around the sample. This reduced by a factor of  $\sim 10$  the recording efficiency of the detector for neutrons scattered by the sample;
- (d) A 0.6 cm thick lead filter was used around the sample; this reduced the constant background by a factor of 2-3 by lowering the efficiency of recording the "soft" gamma rays formed as a result of intensive alpha decay of nuclei in the sample.

As a result of these measures, the total background in the recording channel for radiative-capture events in the 10-30 keV energy range was reduced from  $\sim 50\%$  (1968) to  $\sim 30\%$  for  $^{235}\text{U}$  and from  $\sim 70\%$  (1968) to  $\sim 40\%$  for  $^{239}\text{Pu}$ . The total background in the fission-event recording channel in the same energy range was reduced by  $\sim 30\%$  in the case of  $^{235}\text{U}$  and  $^{239}\text{Pu}$ .

The results obtained agree, within the error limits, with those published earlier (1968); however, in the 2-7 keV energy range the  $\alpha(E)$  values for  $^{239}\text{Pu}$  are systematically higher by  $\sim 30-50\%$ .



Table 1. Averaged values of  $\langle \alpha(E) \rangle$  for  $^{235}\text{U}$

$\Delta E$ eV	$\langle \alpha(E) \rangle$	$\Delta E$ eV	$\langle \alpha(E) \rangle$
100 - 200	0,776 $\pm$ 0,073	3000 - 4000	0,480 $\pm$ 0,050
200 - 300	0,538 $\pm$ 0,050	4000 - 5000	0,421 $\pm$ 0,043
300 - 400	0,500 $\pm$ 0,049	5000 - 6000	0,267 $\pm$ 0,029
400 - 500	0,374 $\pm$ 0,036	6000 - 7000	0,340 $\pm$ 0,033
500 - 600	0,253 $\pm$ 0,026	7000 - 8000	0,287 $\pm$ 0,032
600 - 700	0,426 $\pm$ 0,043	8000 - 9000	0,332 $\pm$ 0,037
700 - 800	0,351 $\pm$ 0,034	9000 - 10000	0,203 $\pm$ 0,021
800 - 900	0,301 $\pm$ 0,037	10000 - 15000	0,334 $\pm$ 0,040
900 - 1000	0,458 $\pm$ 0,043	15000 - 20000	0,370 $\pm$ 0,045
1000 - 2000	0,352 $\pm$ 0,037	20000 - 25000	0,373 $\pm$ 0,047
2000 - 3000	0,400 $\pm$ 0,041	25000 - 30000	0,347 $\pm$ 0,048

Table 2. Averaged values of  $\langle \alpha(E) \rangle$  for  $^{239}\text{Pu}$

$\Delta E$ eV	Sample thickness n nuclei/barn					$\langle \alpha(E) \rangle$
	$8,7 \cdot 10^{-4}$	$5,8 \cdot 10^{-4}$	$2,85 \cdot 10^{-4}$	$1,42 \cdot 10^{-3}$	$2,7 \cdot 10^{-3}$	
100 - 200	0,82±0,21	1,01±0,24	0,86±0,14	0,85±0,17	0,69±0,13	0,85±0,11
200 - 300	0,96±0,24	1,09±0,26	1,02±0,16	1,09±0,21	0,86±0,14	1,00±0,10
300 - 400	0,95±0,26	1,11±0,31	1,09±0,17	1,14±0,22	0,70±0,15	1,00±0,18
400 - 500	0,98±0,29	0,92±0,23	0,89±0,15	0,91±0,18	0,75±0,13	0,89±0,09
500 - 600	0,92±0,23	0,89±0,27	0,82±0,13	0,85±0,17	0,71±0,12	0,84±0,08
600 - 700	1,02±0,20	1,21±0,36	1,73±0,24	2,05±0,40	1,18±0,13	1,44±0,45
700 - 800	1,46±0,39	1,19±0,33	1,17±0,19	1,42±0,27	1,29±0,12	1,31±0,13
800 - 900	1,36±0,36	0,97±0,29	1,17±0,19	1,21±0,23	1,02±0,14	1,15±0,16
900 - 1000	1,35±0,37	1,06±0,32	1,16±0,18	1,43±0,28	1,03±0,13	1,21±0,18
1000 - 2000	1,15±0,22	0,96±0,29	1,06±0,17	1,19±0,23	0,85±0,14	1,04±0,13
2000 - 3000	1,34±0,25	1,01±0,26	1,17±0,19	1,08±0,26	0,87±0,17	1,09±0,18
3000 - 4000	0,95±0,21	0,79±0,20	1,09±0,18	1,11±0,22	0,86±0,15	0,96±0,14
4000 - 5000	0,80±0,19	0,70±0,21	0,77±0,14	0,85±0,18	0,78±0,13	0,78±0,05
5000 - 6000	1,02±0,24	0,76±0,18	0,88±0,17	0,83±0,18	0,63±0,14	0,82±0,14
6000 - 7000	1,07±0,21	0,61±0,17	0,68±0,14	0,72±0,16	0,69±0,12	0,75±0,16
7000 - 8000	0,88±0,22	0,58±0,15	0,45±0,11	0,46±0,13	0,65±0,11	0,60±0,17
8000 - 9000	0,62±0,20	0,43±0,12	0,46±0,11	0,51±0,16	0,43±0,10	0,50±0,07
9000 - 10000	0,44±0,18	0,51±0,14	0,50±0,13	0,39±0,15	0,32±0,11	0,43±0,08
10000 - 20000	0,34±0,15	0,40±0,13	0,41±0,14	0,33±0,11	0,39±0,10	0,37±0,05

Table 3. Comparison of average cross-sections  $\langle \sigma_f(E) \rangle$  for  $^{235}\text{U}$

$\Delta E$ , eV	$\langle \sigma_f(E) \rangle$ Dubna	$\langle \sigma_f(E) \rangle$ ORNL	$\langle \sigma_f(E) \rangle$ Saclay
10 - 20	46,09	-	48,62
20 - 30	35,05	-	35,66
30 - 40	52,12	52,20	50,48
40 - 50	32,21	31,91	30,88
50 - 60	51,10	62,55	55,74
60 - 70	17,88	15,13	16,21
70 - 80	30,37	34,24	29,22
80 - 90	25,68	28,65	25,63
90 - 100	23,00	21,91	23,98
100 - 200	21,39	21,56	21,31
200 - 300	20,83	21,75	20,52
300 - 400	13,11	13,21	14,38
400 - 500	12,98	14,69	13,19
500 - 600	15,00	15,43	14,59
600 - 700	12,00	11,48	11,72
700 - 800	11,10	10,99	10,89
800 - 900	8,93	7,82	8,59
900 - 1000	8,74	7,93	7,87
1000 - 2000	7,84	7,65	7,55
2000 - 3000	5,70	5,46	5,76
3000 - 4000	4,88	4,72	4,89
4000 - 5000	4,54	4,01	4,50
5000 - 6000	3,79	3,46	4,27
6000 - 7000	3,56	3,15	3,79
7000 - 8000	2,65	3,03	3,55
8000 - 9000	3,25	3,03	3,51
9000 - 10000	3,45	3,25	3,42
10000 - 15000	3,14	2,77	2,80
15000 - 20000	2,81	-	-
20000 - 25000	2,60	-	-
25000 - 30000	2,42	-	-

Table 4. Comparison of resonance integrals  $\int \sigma_f(E) \frac{dE}{E}$  barn for  $^{235}\text{U}$

$\Delta E$ eV	Dubna (1964)		Present work	Harwell (1966)	Saclay (1965)	Saclay (1965)	Institute of Atomic Energy (1966)	ORNL (1967)	ORNL (1967)
0,15 - 0,35	145,1			149,1					
0,35 - 0,45	28,6	28,2		30,4					
0,45 - 0,50	8,8	8,6		10,7	9,45			9,3	
0,50 - 0,55	6,9	7,2		7,0	7,59			7,46	
0,55 - 0,70	15,0	14,8		15,4	16,07			15,26	
0,70 - 1,00	19,6	19,2		20,1	20,49			20,33	
1,0 - 1,3	18,0	17,4		18,8	18,88		20,54	18,76	
1,3 - 1,8	5,6	5,5	5,8	5,2	5,86		5,55	5,59	
1,8 - 4,5	16,0	14,9	16,39	14,9	15,74		16,36	15,81	
4,5 - 5,0	0,88	0,84	0,89	0,8	0,8		0,85	0,8	
5,0 - 7,4	8,9	8,2	9,7	9,0	9,7		10,49	9,8	
7,4 - 10,0			21,93	22,6	24,3	23,83	26,12	24,7	
10,0 - 15,0			15,99	15,7	17,4	16,93	18,03	17,2	
15,0 - 20,5			15,27	15,1	16,9	15,60	17,07	17,1	
20,5 - 33,0			16,19	16,3	18,0	16,76	19,1	16,4	17,51
33,0 - 41,0			12,79	11,6	13,5	12,32	15,2	13,8	13,68
41,0 - 60			15,87	16,3		16,43	19,9	17,9	18,12
60 - 73			4,56	3,7		4,5	5,1		4,59
73 - 100			8,07	6,8		7,4	8,9		7,81
100 - 113			2,22	1,8		2,2	2,3		2,05
113 - 200			12,05	10,7					12,52
200 - 300			8,33			8,4			8,51
300 - 1000			14,61			14,9			14,75
1000 - 3000			7,61			7,6			7,7
3000 - 10000			4,72			5,1			5,0
10000 - 20000			2,09			1,9			3,3
20000 - 30000			1,14						

Table 5. Comparison of integral fission cross-sections  $\int \sigma_f(E)dE$  barn eV for  $^{235}\text{U}$

$\Delta E$ eV	Dubna (1964)	Present work	Harwell (1966)	Saclay (1965)	Saclay (1965)	Inst. of Atomic Energy (1966)	ORNL (1967)	ORNL (1967)	Geel (1968)	Geel (1968)	
0,15 - 0,35	34,82		34,58								
0,35 - 0,45	10,97	11,13	11,63								
0,45 - 0,50	4,19	4,09	4,96	4,47			4,39				
0,50 - 0,55	3,60	3,79	3,65	3,97			3,9				
0,55 - 0,70	9,14	9,11	9,35	9,96			9,41				
0,70 - 1,00	16,99	16,1	16,73	17,25			17,04				
1,0 - 1,3	19,58	19,56	21,0	21,16		22,98	20,95				
1,3 - 1,8	8,5	8,27	8,85	7,9	8,83		8,38	8,45			
1,8 - 4,5	47,2	43,6	48,0	44,0	46,49		48,81	46,52			
4,5 - 5,0	4,1	3,9	4,3	3,5	3,8		4,09	4,1			
5,0 - 7,4	56,3	51,3	61,6	57,0	61,4		66,41	62,1			
7,4 - 10,0			195,3	201,0	216,4	212,4	233,0	219,2	210,1	210,2	
10,0 - 15,0			200,9	197,7	218,7	213,0	226,9	216,7	202,9	206,3	
15,0 - 20,5			280,4	278,8	310,9	286,8	326,5	315,6	291,4	290,7	
20,5 - 33,0			415,0	417,0	459,8	427,1	487,2	415,6	447,2	411,2	421,0
33,0 - 41,0			461,8	416,0	484,0	445,0	548,0	495,0	492,0	471,7	476,0
41,0 - 60			808,1	830,0		839,0	1015,0	918,0	925,0	843,1	860,0
60 - 73			306,4	250,0		301,0	348,0		310,0	288,6	290,4
73 - 100			657,9	580,0		631,0	750,0		666,0	613,8	614,5
100 - 113			236,9	184,0		230,0	247,0		216,0	199,8	193,0
113 - 200			1821,3	1589,0		1798,0			1876,0	1750,5	1642,0
200 - 300			2058,1			2059,0			2082,0	1767,9	

Table 5 (continued)

$\Delta E$ eV	Dubna (1964)	Present work	Harwell (1966)	Saclay (1965)	Saclay (1965)	Inst. of Atomic Energy (1966)	ORNL (1967)	(1967)	Geel (1968)	(1968)
300 - 1000		8129,7				8106,0		8106,0	6974,0	
1000 - 3000		13241,4				13310,0		13220,0	13278,0	
3000 - 10000		26665,0				27850,0		27370,0		
10000-20000		30914,0				26690,0		46840,0		
20000-30000		25774,0								

Table 6. Comparison of average cross-sections  $\langle \sigma_f(E) \rangle$  for  $^{239}\text{Pu}$

$\Delta E$ eV	$\langle \sigma_f(E) \rangle$ Dubna	$\langle \sigma_f(E) \rangle$ ANL	$\langle \sigma_f(E) \rangle$ Saclay	$\langle \sigma_f(E) \rangle$ LOS ALAMOS
5,5 - 10,0	26,2	-	-	-
10,0 - 20,0	91,8	103,8	-	-
20,0 - 30,0	26,4	32,8	36,5	42,1
30,0 - 40,0	3,5	3,8	2,7	2,2
40,0 - 50,0	19,0	26,1	28,5	24,6
50,0 - 60,0	50,8	71,8	77,4	72,3
60,0 - 70,0	46,6	53,8	64,0	54,9
70,0 - 80,0	47,6	63,5	70,2	59,5
80,0 - 90,0	61,9	66,4	80,4	61,5
90,0 - 100,0	31,4	27,7	37,4	26,1
100,0 - 200,0	18,1	19,6	21,7	17,8
200,0 - 300,0	17,8	17,5	20,8	16,8
300,0 - 400,0	5,8	9,8	12,9	16,8
400,0 - 500,0	3,7	10,1	10,6	16,8
500,0 - 600,0	16,4	10,8	16,1	20,4
600,0 - 700,0	4,6	3,7	5,3	21,0
700,0 - 800,0	6,1	5,5	6,4	27,1
800,0 - 900,0	6,1	6,2	6,0	33,1
900,0 - 1000,0	8,5	7,7	8,1	39,6
1000 - 2000	4,9	4,0	5,4	6,2
2000 - 3000	3,2	3,4	3,9	2,6
3000 - 4000	3,1	3,5	3,4	2,7
4000 - 5000	2,6	2,7	2,9	2,3
5000 - 6000	1,8	2,8	3,2	2,7
6000 - 7000	1,9	2,7	-	2,2
7000 - 8000	2,1	1,9	-	2,2
8000 - 9000	2,0	2,1	-	2,5
9000 - 10000	1,8	2,3	-	2,1
10000 - 15000	1,5	3,1	-	2,2
15000 - 20000	1,6			

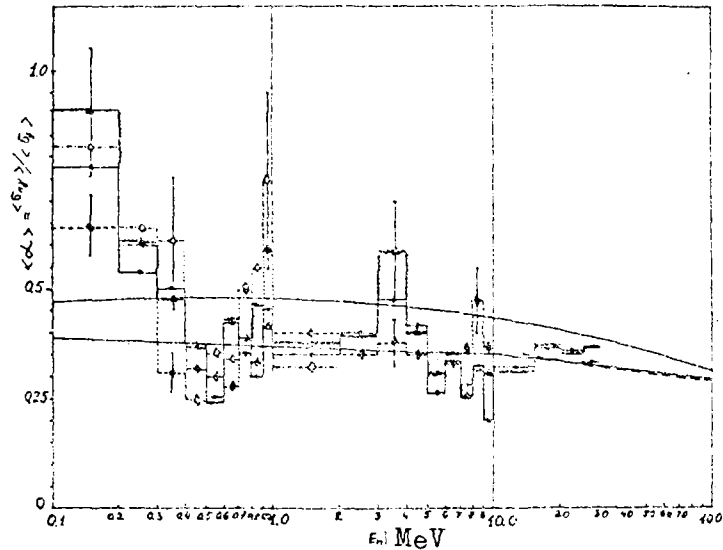


Fig. 1. Measurements of the value of  $\langle \alpha \rangle$  for  $^{235}\text{U}$  in the 0.1-100 keV range.

- . - data of the present work.
- $\text{wavy lines}$  data of authors' 1968 work.
- . -  $\diamond$  - . - data of Gwin et al.
- -  $\diamond$  - - data obtained by subtracting  $\langle \sigma_f(E) \rangle$  of A. Michaudon from total cross-sections  $\langle \sigma_t(E) \rangle$  of James et al.
- - - - data obtained in measurements in electrostatic generators BNL 325, Suppl. 2.

Continuous curves represent calculation by the channel theory ( Y. Kikuchi et al.).



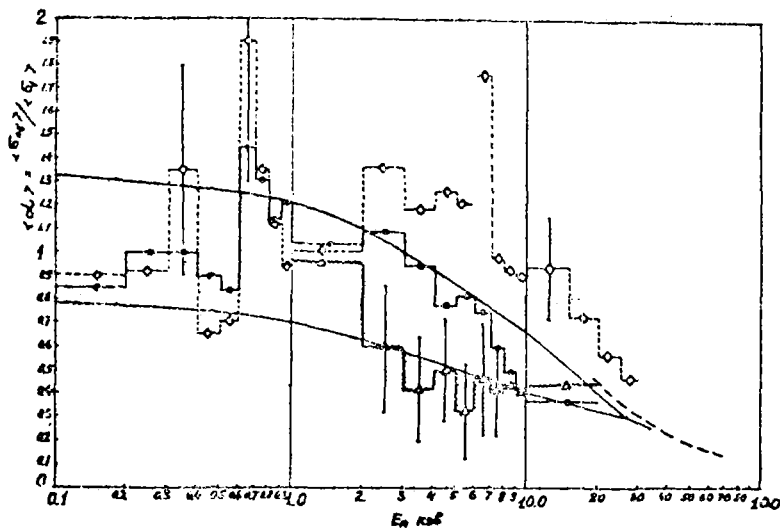


Fig. 2. Measurements of the value of  $\langle \alpha \rangle$  for  $^{239}\text{Pu}$  in the 0.1-100 keV range.

- . - data of present work.
  - $\Delta$  data of authors' 1968 work.
  - - -  $\diamond$  - - - data of M. Sowerby et al.
  - - - - data obtained in measurements in electrostatic generators, BNL-325, Suppl. 2
- Continuous curves represent calculation by the channel theory (Y. Kikuchi et al.).

ALPHA-PARTICLE SPECTRA OF THE DECAY OF  
RESONANCE STATES OF  $^{146}\text{Nd}$

Yu.P. Popov, M. Pshitula, K.G. Rodionov,  
R.F. Rumi, M. Stempinski and V.I. Furman

(Preprint JINR R3-5073, 1970)

The paper presents the results of the first measurements of alpha particle spectra in the  $^{145}\text{Nd}(n,\alpha)^{142}\text{Ce}$  reaction. The studies were performed in a neutron beam from an IBR pulsed reactor, use having been made of a grid-type double ionization chamber.

In the case of resonance states with  $E_0 = 4.36$  and  $43.1$  eV, the partial alpha widths of transitions to the ground and first excited states of the daughter nucleus (Table 1.) were determined.

On the basis of these and other data for a number of nuclei, the average values of the reduced neutron and alpha widths were compared. The comparison indicates the approximative nature of the Bethe hypothesis that these widths are equal (Table 2.).

Table 1. Reduced alpha widths of the decay of the neutron resonance states of  $^{146}\text{Nd}$  with  $E_0 = 4.36$  and  $43.1$  eV to the ground and first excited states.

Resonance, $E_0$ , eV	$E_{\text{excit.}}$ MeV	$I^{\pi}$	$N_{\alpha}$	$\Gamma_{\alpha i}$ , meV	$\sum_i \Gamma_{\alpha i} \cdot 10^7$	$\bar{\Gamma}_{\alpha i}^2$ eV
4,36	0	$0^+$	$409 \pm 21$	$0,26 \pm 0,07$	2,54	0,5
	0,65	$2^+$	$267 \pm 17$	$0,17 \pm 0,05$	0,60	1,4
4,31	0	$0^+$	$128 \pm 12$	$0,12 \pm 0,04$	2,54	0,24
	0,65	$2^+$	$19 \pm 7$	$0,02 \pm 0,01$	0,60	0,17

Table 2. Comparison of the reduced neutron and partial alpha widths

Target nucleus	<sup>95</sup> SrO [12]	<sup>123</sup> Te [12]	<sup>143</sup> Nd [10]	<sup>145</sup> Nd	<sup>145</sup> Sm [2]	<sup>148</sup> Sm [4]	<sup>153</sup> Gd [6]
$\overline{\gamma_n^2}$	4,3	1,9	5,0	1,9	1,9	1,2	0,23
$\overline{\gamma_n^2} (N)$	0,21(5)	0,5(4)	0,8(5)	0,5(4)	0,08(9)	0,007(6)	0,005(2)
$\overline{\gamma_n^2} / \overline{\gamma_n^2}$	0,05	0,26	0,16	0,32	0,042	0,006	0,02

N is the number of alpha transitions for which  $\overline{\gamma_n^2}$  was averaged.

RADIUM INSTITUTE OF THE ACADEMY OF SCIENCES

THE KINETIC ENERGIES OF FRAGMENTS AND THE ANGULAR DISTRIBUTIONS  
OF ALPHA PARTICLES IN SPONTANEOUS TERNARY FISSION OF  $^{252}\text{Cf}$

V.M. Adamov, L.V. Drapchinskii, S.S. Kovalenko,  
K.A. Petrzhak and T.I. Tyutyugin

(Submitted to *Jadernaja Fizika*)

Measurements were made of the correlations between the average values of the kinetic energies of fragments and alpha particles and between the energy of alpha particles and their angles of emission in relation to the direction of fragment motion in spontaneous  $^{252}\text{Cf}$  fission. The fragments and alpha particles were recorded by means of silicon detectors. The correlations between the average kinetic energy of fragments  $\bar{E}_k$ , average kinetic energy of light  $\bar{E}_l$  and heavy  $\bar{E}_h$  groups of fragments and the energy of alpha particles  $E_\alpha$  are, respectively

$$\frac{\Delta \bar{E}_k}{\Delta E_\alpha} = -(0.30 \pm 0.05), \quad \frac{\Delta \bar{E}_l}{\Delta E_\alpha} = -(0.14 \pm 0.02), \quad \frac{\Delta \bar{E}_h}{\Delta E_\alpha} = -(0.16 \pm 0.04)$$

in the alpha-particle energy range from 10 to 26 MeV. The shift of the average kinetic energy of ternary fission fragments as compared with that of binary fission fragments is  $\Delta E_k = (11.7 \pm 1.3)$  MeV; the shifts of the average kinetic energy of the light  $\Delta \bar{E}_l$  and heavy  $\Delta \bar{E}_h$  groups of fragments are equal to  $(7.3 \pm 0.9)$  MeV and  $(4.4 \pm 0.9)$  MeV, respectively. The angular distributions of the alpha particles are approximated by Gaussian distributions with a most probable angle of emission of  $92^\circ$  relative to the direction of fragment motion and standard deviations  $(13.2 \pm 0.7)^\circ$ ,  $(13.5 \pm 0.7)^\circ$ ,  $(16.2 \pm 0.7)^\circ$ , and  $(27.5 \pm 1.0)^\circ$  for alpha particle energies in the 13-16, 16-20, 20-24 and above 24 MeV ranges. The maximum of the alpha-particle energy distributions shifts towards higher energies by 5 MeV when the angle changes from  $90^\circ$  to  $45^\circ$ , and the relative number of high-energy alpha particles increases.

RADIOCHEMICAL DETERMINATION OF ABSOLUTE FRAGMENT YIELDS  
IN  $^{239}\text{Pu}$  AND  $^{241}\text{Pu}$  FISSION BY SLOW NEUTRONS, BY  
MEANS OF MICA DETECTORS FOR MEASURING THE  
NUMBER OF FISSIONS

V. Sorokina, N.V. Skovorodkin, S.S. Bugorkov,  
A.S. Krivokhatsky and K.A. Petrzhak

The radiochemical method was used to obtain the absolute cumulative yields of  $^{99}\text{Mo}$ ,  $^{140}\text{Ba}$ ,  $^{141}\text{Ce}$  and  $^{144}\text{Ce}$  in  $^{239}\text{Pu}$  and  $^{241}\text{Pu}$  fission by slow neutrons. The number of fissions in the sample was determined directly from the number of fissions in a small aliquot of fissionable substance applied on a mica detector and irradiated simultaneously with the main sample in the same neutron flux. The absolute activity of the radionuclides under study was measured in a  $4\pi$   $\beta$  counter. The yields of  $^{99}\text{Mo}$ ,  $^{141}\text{Ce}$  and  $^{144}\text{Ce}$  in  $^{239}\text{Pu}$  fission were  $6.17 \pm 0.19$ ,  $5.18 \pm 0.13$  and  $3.85 \pm 0.09\%$  respectively and those of  $^{99}\text{Mo}$ ,  $^{140}\text{Ba}$ ,  $^{141}\text{Ce}$  and  $^{144}\text{Ce}$  in  $^{241}\text{Pu}$  fission  $6.15 \pm 0.16$ ,  $5.64 \pm 0.11$ ,  $4.81 \pm 0.14$  and  $4.08 \pm 0.14\%$  respectively. The errors in determining the yields of these elements does not exceed  $\pm 5\%$ . The yields measured are compared with values given in the literature. Earlier measurements of the cumulative yields of 17 rare-earth elements and  $^{91}\text{Y}$  in relation to the cumulative yield of  $^{144}\text{Ce}$  were used to calculate the absolute yields of these elements in  $^{239}\text{Pu}$  and  $^{241}\text{Pu}$  fission by slow neutrons:

$^{141}\text{La}$  -  $4.70 \pm 0.26$  and  $4.50 \pm 0.17$ ,  $^{141}\text{Ce}$  -  $5.09 \pm 0.14$  and  $4.78 \pm 0.18$ ,  
 $^{143}\text{Ce}$  -  $3.99 \pm 0.21$  and  $3.88 \pm 0.16$ ,  $^{143}\text{Pr}$  -  $4.27 \pm 0.17$  and  $4.31 \pm 0.15$ ,  
 $^{145}\text{Pr}$  -  $3.54 \pm 0.16$  and  $3.01 \pm 0.14$ ,  $^{147}\text{Nd}$  -  $2.13 \pm 0.09$  and  $2.34 \pm 0.09$ ,  
 $^{147}\text{Pm}$  -  $2.14 \pm 0.13$  and  $2.35 \pm 0.12$ ,  $^{149}\text{Nd}$  -  $1.14 \pm 0.08$  and  $1.47 \pm 0.06$ ,  
 $^{149}\text{Pm}$  -  $1.30 \pm 0.05$  and  $1.52 \pm 0.08$ ,  $^{151}\text{Pm}$  -  $0.741 \pm 0.036$  and  $0.846 \pm 0.050$ ,  
 $^{153}\text{Sm}$  -  $0.370 \pm 0.015$  and  $0.522 \pm 0.022$ ,  $^{155}\text{Eu}$  -  $0.171 \pm 0.019$  and  $0.231 \pm 0.022$ ,  
 $^{156}\text{Sm}$  -  $0.121 \pm 0.005$  and  $0.163 \pm 0.007$ ,  $^{156}\text{Eu}$  -  $0.124 \pm 0.005$  and  $0.170 \pm 0.006$ ,  
 $^{157}\text{Eu}$  -  $0.0764 \pm 0.0037$  and  $0.130 \pm 0.006$ ,  $^{159}\text{Gd}$  -  $0.0216 \pm 0.0007$  and  $0.0462 \pm 0.0018$ ,  
 $^{161}\text{Tb}$  -  $0.00515 \pm 0.0020$  and  $0.00815 \pm 0.000326$ ,  $^{91}\text{Y}$  -  $2.46 \pm 0.08$  and  $1.67 \pm 0.06$ .

MASS-SPECTROMETRIC DETERMINATION OF THE RELATIVE YIELDS  
OF XENON ISOTOPES IN THE FISSION OF NATURAL  
URANIUM BY 14.7-MeV NEUTRONS

K.A. Petrzak, V.F. Teplikh and M.G. Panyan

(Published in Bjulleten' CJaD GKAE, No. 6 (1969))

The relative yields of xenon isotopes in  $^{238}\text{U}$  fission by neutrons with an energy of 14.7 MeV were measured in a high-sensitivity mass spectrometer.

The fine structure of the yield curve was found to be in the region of mass 134, as in  $^{238}\text{U}$  fission by fission-spectrum neutrons. Contrary to the widely held view that the yield curve becomes smooth with increasing excitation energy of the fissionable nucleus, it is shown that an increase in the excitation energy of  $^{239}\text{U}$  from 7.7 to 18.9 MeV leads to a more pronounced fine-structure peak.

INSTITUTE OF PHYSICS  
ACADEMY OF SCIENCES OF THE UKRAINIAN SSR

TEMPERATURE DEPENDENCE OF THE CROSS-SECTIONS FOR SCATTERING  
OF COLD AND THERMAL NEUTRONS BY O<sub>2</sub> AND D<sub>2</sub> MOLECULES

V.P. Vertebny, V.A. Gulko, A.N. Maistrenko, N.N. Matviishina  
and V.F. Razbudei

(Submitted to Ukrainskij Fizičeskij Žurnal)

An experimental study was undertaken of the total cross-sections for neutron scattering by diatomic oxygen and deuterium molecules as a function of temperature in the 1-8 Å neutron wave-length region. Deuterium and oxygen are the simplest of molecular systems, i.e. they are diatomic. With computers, the case of diatomic molecules can be dealt with easily by the procedure described in Refs [1, 2], which give detailed cross-section data, thus providing a means for verifying the theory of slow-neutron scattering by molecules.

The total neutron cross-sections were measured by the transmission method using the time-of-flight technique in the horizontal channel of a VVR-M reactor. The unit had a resolution of 15 μsec/m. The samples were used in gaseous form at a pressure of 8-12 atm. The purity of the gases, according to the manufacturers' data was: deuterium 99.62% and oxygen 99%. Sample thickness along the beam: deuterium  $3.36 \times 10^{22}$  nuclei/cm<sup>2</sup> and oxygen  $4.56 \times 10^{22}$  nuclei/cm<sup>2</sup>. The total cross-sections were measured at sample temperatures of 173, 223, 293, 323 and 373°K. The temperature stabilization system enabled the sample temperature to be maintained to within  $\pm 1^\circ\text{C}$ .

The experimental data for the scattering cross-sections as a function of  $\lambda$  are shown in Tables 1 and 2. The total cross-sections for neutron scattering by oxygen and deuterium molecules were calculated by the Young and Koppel theory [1] so that they could be compared with the experimental data. The total cross-sections are obtained by integrating the doubly differentiated scattering cross-sections with respect to energy transfer  $\epsilon$  and solid angle  $\Omega$ . The calculation was performed on the M-20 computer. The results are shown in Figs 1 and 2.

In calculating the cross-sections for oxygen, paramagnetic scattering was taken into account. It was calculated by the formula

$$\sigma_{\text{eff}}^{\text{magn}} = \frac{1}{\Omega} \left( \frac{\mu}{2\pi k_B T} \right)^2 \int_0^\infty \sigma^{\text{magn}}(\omega) \omega^2 \left[ e^{-\frac{\hbar\omega}{k_B T}} (v-\omega)^2 - e^{-\frac{\hbar\omega}{k_B T}} (v+\omega)^2 \right] d\omega$$



where  $v$  is the relative neutron and molecule velocity and  $u$  neutron velocity in the laboratory system of co-ordinates. The cross-section for magnetic scattering  $\sigma^{\text{mag}^n}(v)$  by an oxygen molecule at rest is taken from Kleiner [3]. The calculation shows that magnetic scattering by gaseous oxygen is virtually independent of sample temperature in the temperature range under consideration. The calculation results are shown in Table 1a.

The total cross-section for  $O_2$  was calculated by summation of the nuclear part of the scattering cross-section and the magnetic scattering cross-section.

For comparison, calculations were also performed in accordance with the quasi-classical theory of Krieger and Nelkin [4]. The following effective mass values were also used in the calculation:  $D_2 - 4.0128 \times 10^{-24}g$  and  $O_2 - 31.868 \times 10^{-24}g$ . Calculations by both theories gave very similar results for both gases.

#### REFERENCES

- [1] YOUNG, I.A., KOPPEL, I.U., Phys. Rev., 134, A603 (1964).
- [2] LØVSETH, J., Physica Norvegica, 3, 127 (1962).
- [3] KLEINER, W.H., Phys. Rev., 97, 411 (1955).
- [4] KRIEGER, T.J., NELKIN, M., Phys. Rev., 106, 290 (1957).

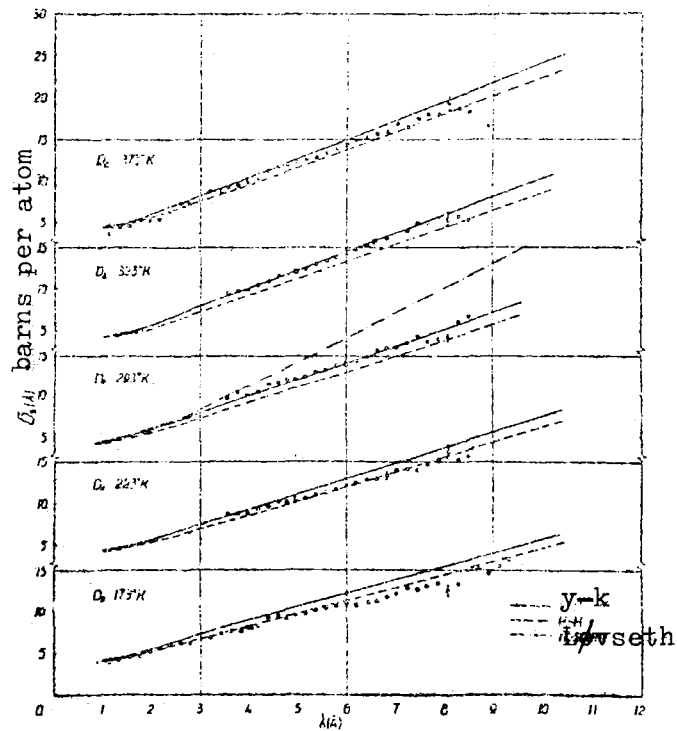


Fig. 1

Total cross-section for scattering by gaseous deuterium

Experiment: Y-K - calculation by the theory of Young and Koppel;

K-N - calculation by the theory of Krieger and Nelkin;

Løvseth - calculation performed by Løvseth.

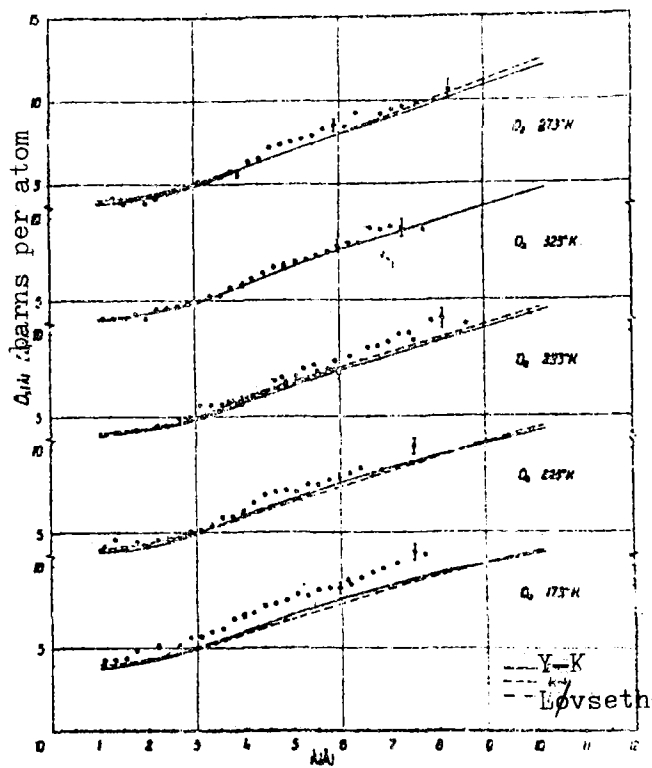


Fig. 2 Total cross-section for scattering by gaseous oxygen

Experiment: Y-K - calculation by the theory of Young and Koppel;

K-N - calculation by the theory of Krieger and Nelkin;

Løvseth - calculation performed by Løvseth.

Table 1a

$\lambda$ (Å)	$\sigma^s$ magn (barn)				
	173°K	223°K	293°K	323°K	373°K
1	0,130	0,130	0,130	0,130	0,130
2	0,483	0,485	0,490	0,490	0,493
3	0,995	0,987	0,981	0,973	0,973
4	1,598	1,557	1,516	1,501	1,475
5	2,149	2,082	2,015	1,989	1,946
6	2,639	2,555	2,500	2,470	2,400
7,5	3,196	3,124	3,054	3,035	3,014
10	3,911	3,887	3,960	3,860	3,952
15	5,407	5,521	5,760	5,692	5,770
20	6,900	7,147	7,320	7,495	7,576
30	9,900	10,432	11,090	11,121	11,291

Table 1

Total cross-sections for neutron scattering by molecular deuterium

$T = 173^\circ\text{K}$		$T = 173^\circ\text{K}$		$T = 223^\circ\text{K}$	
$\lambda$ (Å)	$\sigma$ , (barn/atom)	$\lambda$ (Å)	$\sigma$ , (barn/atom)	$\lambda$ (Å)	$\sigma$ , (barn/atom)
1,11	3,74	5,99	10,55±0,30	3,55	8,54
1,32	3,98	6,20	10,35	3,76	8,55±0,35
1,53	4,29	6,41	10,67	3,97	8,56
1,74	4,45	6,62	10,81	4,18	9,02
1,95	4,92±0,10	6,83	11,32	4,39	9,38
2,16	5,34	7,04	11,70	4,60	9,94
2,37	5,68	7,25	12,39	4,77	9,80
2,58	5,92	7,46	12,17	4,95	10,09±0,50
2,79	5,89	7,66	12,60	5,16	10,24
3,00	6,32	7,87	12,95	5,37	10,68
3,21	6,52	8,08	12,01±0,50	5,58	11,03
3,41	7,02	8,29	12,79	5,78	11,28
3,62	7,22	8,71	14,75	5,99	11,75
3,83	7,29	8,92	14,15	6,20	12,11
3,97	7,76±0,10	9,13	15,03	6,41	12,46
4,18	7,91	9,34	15,79	6,62	12,56
4,39	8,83			6,83	12,96±0,45
4,60	9,13			7,04	13,63
4,77	8,77			7,25	13,69
4,95	9,16			7,46	13,54
5,16	9,32			7,67	14,27
5,37	9,68			7,87	14,82
5,58	9,96			8,08	15,72±0,85
5,78	10,26			8,29	14,73
				8,50	15,21

Table 1 (contd.)

$T = 293^{\circ}\text{K}$		$T = 323^{\circ}\text{K}$		$T = 373^{\circ}\text{K}$	
$\lambda$ (Å)	$\sigma$ (barn) atom	$\lambda$ (Å)	$\sigma$ (barn) atom	$\lambda$ (Å)	$\sigma$ (barn) atom
3,55	9,28	3,55	9,26	1,11	3,46
3,76	10,06	3,76	9,55	1,33	4,27
3,97	9,63 $\pm$ 0,10	3,97	9,47 $\pm$ 0,10	1,53	4,38
4,18	10,08	4,18	10,21	1,74	5,08
4,39	10,97	4,39	10,71	1,95	5,05
4,60	11,24	4,60	11,30	2,16	5,19
4,77	11,54	4,77	11,42	2,37	6,05
4,95	11,69	4,95	11,72 $\pm$ 0,20	2,58	7,07
5,16	12,03	5,16	12,14	2,79	7,02
5,37	12,59	5,37	12,57	3,00	7,56
5,58	12,87	5,58	13,02	3,21	8,55
5,78	13,37	5,78	13,42	3,42	8,45
5,99	13,55 $\pm$ 0,25	5,99	13,87 $\pm$ 0,30	3,55	9,04
6,20	13,88	6,20	14,32	3,76	9,20
6,41	14,42	6,41	14,73	3,97	9,56 $\pm$ 0,10
6,62	15,22	6,62	15,42	4,18	10,00
6,83	15,43	6,83	15,69	4,39	10,93
7,04	15,55	7,04	15,77	4,60	11,45
7,25	16,14	7,25	16,49	4,77	11,54
7,46	16,92	7,46	17,46	4,95	11,92
7,67	16,23	7,67	17,53	5,16	12,27
7,87	15,53	7,87	16,80	5,37	12,45
8,08	16,71 $\pm$ 0,50	8,08	17,82 $\pm$ 0,90	5,58	13,02
8,29	18,57	8,29	18,13	5,78	13,63
8,50	19,16	8,50	17,72	5,99	13,92 $\pm$ 0,23
				6,20	14,43
				6,41	14,89
				6,62	15,25
				6,83	15,50
				7,04	16,45
				7,25	16,04
				7,46	17,10
				7,67	17,57
				7,87	17,58
				8,08	18,85 $\pm$ 0,80
				8,29	18,24
				8,50	17,72

Table 2

Total cross-sections for neutron scattering by molecular oxygen

$T = 173^{\circ}\text{K}$		$T = 223^{\circ}\text{K}$		$T = 293^{\circ}\text{K}$	
$\lambda$ (Å)	$\sigma$ , (barn/atom)	$\lambda$ (Å)	$\sigma$ , (barn/atom)	$\lambda$ (Å)	$\sigma$ , (barn/atom)
1,11	4,23±0,04	1,11	4,14±0,04	1,77	4,22
1,33	4,27	1,33	4,55	1,99	4,25±0,08
1,55	4,35	1,55	3,99	2,21	4,44
1,77	4,82	1,77	4,41	2,44	4,43
1,99	4,22	1,99	4,12	2,66	4,92
2,21	5,15	2,21	4,53	2,88	4,96±0,10
2,44	4,56	2,44	4,63	3,10	5,70
2,66	5,14	2,66	4,68	3,32	5,72
2,88	5,60±0,10	2,88	4,98±0,08	3,54	5,75
3,10	5,69	3,10	5,12	3,69	5,93
3,32	5,93	3,32	5,41	3,77	5,97
3,54	6,14	3,54	5,89	3,99	5,94±0,30
3,77	6,78	3,76	5,96	4,06	5,97
3,99	6,97±0,14	3,99	6,16±0,17	4,21	6,28
4,21	7,09	4,21	6,80	4,43	6,22
4,43	7,53	4,43	7,29	4,65	7,19
4,65	7,66	4,65	7,44	4,80	7,38
4,87	7,89	4,87	7,52	4,87	7,08
5,02	8,11	5,10	7,45	5,10	7,48
5,10	8,27	5,32	7,89	5,24	7,90
5,32	8,14	5,54	7,90	5,46	8,13
5,54	8,51	5,76	8,14	5,54	7,74
5,76	8,65	5,98	8,25±0,30	5,76	7,97
5,98	8,62±0,40	6,20	8,52	5,91	8,38±0,20
6,20	8,86	6,42	8,87	5,98	7,60±0,40
6,42	9,23	6,65	8,33	6,20	8,65
6,65	9,58	6,87	8,72	6,56	9,15
6,87	9,81	6,98	9,71±0,50	6,79	9,27
7,16	10,12	7,53	10,18±0,50	7,02	9,50
7,53	10,82±0,50			7,24	10,01
7,75	10,68			7,46	10,57
				7,53	9,64
				7,90	10,77
				8,12	10,96±0,70
				8,62	10,57

Table 2 (contd.)

$T = 323^{\circ}\text{K}$		$T = 373^{\circ}\text{K}$	
$\lambda(\text{\AA})$	$\sigma$ , barn/atom	$\lambda(\text{\AA})$	$\sigma$ , barn/atom
I,II	$3,91 \pm 0,04$	I,II	$3,78 \pm 0,05$
I,33	3,91	I,33	4,17
I,55	3,95	I,55	3,80
I,77	4,15	I,77	4,12
I,99	3,88	I,99	3,83
2,21	4,43	2,21	4,12
2,44	4,54	2,44	4,47
2,66	$4,56 \pm 0,09$	2,66	$4,56 \pm 0,09$
2,88	4,78	2,88	4,90
3,10	4,94	3,10	5,17
3,32	5,26	3,32	5,24
3,54	5,29	3,54	5,42
3,76	5,76	3,76	5,74
3,99	$6,17 \pm 0,10$	3,91	$5,59 \pm 0,17$
4,21	6,38	4,14	6,38
4,43	6,63	4,36	6,54
4,65	7,00	4,58	7,24
4,87	7,15	4,80	7,41
5,09	7,35	5,02	7,58
5,32	7,41	5,24	7,75
5,54	7,69	5,46	7,97
5,76	7,91	5,68	8,36
5,98	$8,26 \pm 0,40$	5,91	$8,52 \pm 0,40$
6,20	8,46	6,13	8,47
6,42	8,41	6,35	9,24
6,65	$9,34 \pm 0,60$	6,65	$8,60 \pm 0,55$
6,86	9,24	8,86	9,18
7,09	9,49	7,09	9,48
7,31	$9,34 \pm 0,50$	7,31	9,63
7,75	9,24	7,60	9,85
		8,27	$10,61 \pm 0,61$

NEUTRON CROSS-SECTIONS OF THE ISOTOPES

$^{161}\text{Dy}$ ,  $^{162}\text{Dy}$ ,  $^{163}\text{Dy}$  AND  $^{164}\text{Dy}$

V.P. Vetrebny, M.F. Vlasov, N.L. Gnidak, A.L. Kirilyuk,  
E.A. Pavlenko, M.V. Pasechnik, N.A. Trofimova and  
A.F. Fedorova

Table 1 gives the total cross-sections of dysprosium isotopes determined in the VVR-M reactor of the Institute of Physics, Academy of Sciences of the Ukrainian SSR, by the time-of-flight method with a resolution of  $\sim 1.5 \mu\text{sec/m}$  in the 0.03-1.5 eV energy range. The measurements were performed on samples of dysprosium oxide  $\text{Dy}_2\text{O}_3$ . The isotopic composition is given in Table 3. In the processing of the data, corrections were made for magnetic scattering (for  $v = 2200 \text{ m/sec}$  and  $\sigma_{\text{magn}} = 20.3 \text{ barn}$ ) and inhomogeneity of the sample ( $< 1\%$ ). Table 1 gives only the statistical errors. It was shown experimentally that, in the case of dysprosium-164, impurities cannot increase the cross-section by more than 2% and, in the case of dysprosium-162, by more than 8%. The total, capture and scattering cross-sections for  $v = 2200 \text{ m/sec}$  are shown in Table 2. The total and capture cross-sections were obtained by extrapolating the experimental data to this point. The validity of extrapolation is confirmed by the fact that  $\sigma_{\text{p}} \sqrt{E}$  is constant in an energy range much higher than 0.005 eV in the neighbourhood of 0.03 eV. The corrections for resolutions which are associated with the 1.73-eV level of  $^{163}\text{Dy}$  were not applied to the values for 1.5 eV. In Table 2, account is also taken of the errors due to the drift of the apparatus ( $^{161}\text{Dy} \approx 1.5\%$ ,  $^{162}\text{Dy} \approx 1.8\%$ ,  $^{163}\text{Dy} \approx 2.0\%$  and  $^{164}\text{Dy} \approx 1.5\%$ ). In the measurement of total cross-sections, the samples at point  $v = 2200 \text{ m/sec}$  had a thickness of  $n\sigma_t = 1.6, 0.86, 0.68$  and  $2.9$ , respectively, for  $^{161}\text{Dy}$ ,  $^{162}\text{Dy}$ ,  $^{163}\text{Dy}$  and  $^{164}\text{Dy}$ .

The scattering cross-sections had been measured earlier by the authors.



Table 1

Energy dependence of the total neutron cross-sections of dysprosium isotopes

Neutron energy, eV	Total cross-sections of isotopes, barn			
	$Dy^{161}$	$Dy^{162}$	$Dy^{163}$	$Dy^{164}$
1,5	52,0 $\pm$ 3	52,0 $\pm$ 0,7	328 $\pm$ 2	242 $\pm$ 6
1,0	61	41	90	343
0,9	67	43	77	357
0,8	72	40	68	399
0,7	80 $\pm$ 2,5	43 $\pm$ 2	56 $\pm$ 2	463 $\pm$ 7
0,6	87	44	54	517
0,5	106	44	47	601
0,4	125 $\pm$ 4	51 $\pm$ 2	49 $\pm$ 2	691 $\pm$ 8
0,3	153	52	51	832
0,2	201	63	57	1068
0,19	214	65	59	1091
0,18	219 $\pm$ 3	66 $\pm$ 2	60 $\pm$ 1	1125 $\pm$ 8
0,17	226	71	57	1163
0,16	239	73	60	1216 $\pm$ 7
0,15	250	73	64	1250
0,14	259	78 $\pm$ 1	63,5	1305
0,13	270	81	62	1347
0,12	286	86	65 $\pm$ 1	1403 $\pm$ 6
0,11	299	89	68	1463
0,1	315 $\pm$ 2	94 $\pm$ 1	70 $\pm$ 1	1529 $\pm$ 6
0,09	338	100	75	1610
0,08	358	103	79	1713
0,07	389 $\pm$ 2	109 $\pm$ 1	83 $\pm$ 1	1826 $\pm$ 6
0,06	426	115	90	1972
0,05	473 $\pm$ 3	127 $\pm$ 1	95 $\pm$ 1	2171 $\pm$ 8
0,04	536	137	101	2424
0,03	622 $\pm$ 5	159 $\pm$ 2	120 $\pm$ 2	2783 $\pm$ 21
0,0253	677	172	126	3000

Table 2

Neutron constants of dysprosium isotopes for  $v = 2200$  m/sec

Isotope	Total cross-section $\sigma_t$ , in barns	Absorption cross-section $\sigma_a$ , in barns	Scattering cross-section in barns	$\bar{\sigma}_a^{(*)}$
Dy 161	$677^{+12}_{-20}$	$655^{+12}_{-20}$	$22 \pm 1$	$630 \pm 17$
Dy 162	$172^{+6}_{-16}$	$170^{+6}_{-16}$	$2,5 \pm 0,8$	$176^{+6}_{-9}$
Dy 163	$126^{+6}_{-12}$	$116^{+6}_{-12}$	$9,7 \pm 0,4$	$126^{+6}_{-12}$
Dy 164	$3000^{+45}_{-70}$	$2740^{+45}_{-70}$	$262 \pm 7$	$2740^{+45}_{-70}$

$\bar{\sigma}_a^{(*)}$  -- Cross-sections averaged from the authors data and data of other studies.

Table 3

Isotopic composition of samples

Sample	Isotope concentration, %				
	160	161	162	163	164
Dy 161	0,6	94,2	3,5	1,1	0,6
Dy 162	0,2	1,6	94,0	3,3	0,9
Dy 163	0,2	0,4	2,1	92,8	4,5
Dy 164	0,1	0,3	0,8	1,8	97

INSTITUTE OF THEORETICAL AND EXPERIMENTAL PHYSICS

NEUTRON POLARIZATION IN THE D-D REACTION

V.M. Morozov, G.V. Gorlov, Yu.G. Zubov and N.S. Lebedeva

The polarization  $P_p$  of neutrons emitted in the D-D reaction at an angle of  $37^\circ$  in the laboratory system of co-ordinates was measured for four different energies of accelerated deuterons  $E_d$ . The Schwinger scattering of neutrons at small angles by lead and uranium nuclei was used as the polarization analyser.

$E_d$ , MeV	$P_p$ , %
$1.2^{+0.12}$	$-(14.5^{+1.5})$
$2.0^{+0.12}$	$-(13.9^{+1.7})$
$2.4^{+0.12}$	$-(13.0^{+1.6})$
$2.7^{+0.08}$	$-(10.0^{+1.6})$

GORKY POLYTECHNICAL INSTITUTE

ANGULAR ENERGY DISTRIBUTIONS OF GAMMA RADIATION  
FROM A PLANE ISOTROPIC SOURCE BEHIND IRON  
BARRIERS

B.S. Kondratyev

(Published in Bjulleten' CJaD GKAE, No. 6 (1970))

The Monte Carlo method was used for calculating the angular energy distributions of the scattered gamma radiation from a plane isotropic source behind iron barriers of different thicknesses at different initial energies. The angular distributions of the radiation were obtained. The data are presented in the form of tables and graphs which can be used for engineering calculations of radiation protection.

ALL-UNION SCIENTIFIC RESEARCH INSTITUTE OF PHYSICO-  
TECHNICAL AND RADIO TECHNICAL MEASUREMENTS

ACTIVATION DETECTORS FOR NEUTRONS

R.D. Vasilyev, E.A. Grigoryev and V.P. Yaryna

(Submitted to Bjulleten' CJaD GKAE, No. 7 (1971))

The present survey classifies current data on the nuclear-physical characteristics of activation detectors for neutrons. It considers 24 detectors for measurements in the region of thermal and epithermal neutrons and 28 detectors for measurements in the fast neutron region. In the case of the 12 most widely used resonance detectors, the resonance parameters of the activation reactions are discussed in detail.